



CAPACITY OF PEGGED MORTISE AND TENON JOINERY

**Joseph F. Miller
Richard J. Schmidt**

**Department of Civil and
Architectural Engineering
University of Wyoming
Laramie, WY 82071**

A report on research co-sponsored by:

**Timber Frame Business Council
Hamilton, MT**

**Timber Framers Guild
Becket, MA**

**University of Wyoming
Laramie, WY 82071**

February 2004



**UNIVERSITY
OF WYOMING**

REPORT DOCUMENTATION PAGE	1. REPORT NO.	2.	3. Recipient's Accession No.
4. Title and Subtitle Capacity of Pegged Mortise and Tenon Joints		5. Report Date February 2004	
7. Author(s) Joseph F. Miller & Richard J. Schmidt		6.	
9. Performing Organization Name and Address Department of Civil and Architectural Engineering University of Wyoming Laramie, Wyoming 82071		8. Performing Organization Report No.	
12. Sponsoring Organization Name and Address Timber Frame Business Council Timber Framers Guild University of 217 Main Street PO Box 60 Wyoming Hamilton, MT 59840 Becket, MA 01223 Laramie, WY 82071		10. Project/Task/Work Unit No. 11. Contract(C) or Grant(G) No. (C) (G)	
15. Supplementary Notes		13. Type of Report & Period Covered final	
16. Abstract (Limit: 200 words) Traditional timber frames use hardwood pegs to secure mortise and tenon connections, resulting in shear loading of the peg. Despite the historical usage of such connections, no applicable building codes or guidelines are available for engineers and designers to follow. The object of this research is to quantify the shear capacity of wooden pegs in a mortise and tenon joint by both physical testing of full-scale specimens as well as modeling their macroscopic behavior by the finite element method. By testing various species of wood used in both the frame members as well as the pegs, a correlation between shear strength and the specific gravity of the frame materials is developed. This correlation is then used to develop a design method for mortise and tenon joints.		14.	
17. Document Analysis a. Descriptors traditional timber framing, heavy timber construction, structural analysis, wood peg fasteners, mortise and tenon connections, dowel connections, lateral load response, European yield model, b. Identifiers/Open-Ended Terms c. COSATI Field/Group			
18. Availability Statement Release Unlimited		19. Security Class (This Report) unclassified	21. No. of Pages 84
		20. Security Class (This Page) unclassified	22. Price

Acknowledgments

Acknowledgments and thanks are extended to thank Helmsburg Sawmill and Carl Miller for their help in providing the timbers along with the Timber Frame Business Council and the Timber Framers Guild for financial support.

TABLE OF CONTENTS

1.0	INTRODUCTION.....	- 1 -
1.1	HISTORY AND BACKGROUND	- 1 -
1.2	PROBLEM STATEMENT	- 2 -
1.3	LITERATURE REVIEW	- 4 -
1.4	OBJECTIVES AND SCOPE OF WORK	- 7 -
2.0	TESTING PROCEDURES AND RESULTS.....	- 8 -
2.1	JOINT TESTS	- 8 -
2.1.1	<i>Tension Testing</i>	- 8 -
2.1.2	<i>Shear Testing</i>	- 18 -
2.1.3	<i>Direct Bearing Tests</i>	- 23 -
2.2	DOWEL BEARING TESTS.....	- 25 -
3.0	FINITE ELEMENT MODELING	- 27 -
3.1	OBJECTIVES	- 27 -
3.2	MODEL DEVELOPMENT	- 27 -
3.3	RESULTS	- 34 -
3.4	DIRECT BEARING JOINTS	- 38 -
4.0	SPECIFIC GRAVITY AND YIELD STRESS CORRELATION	- 41 -
4.1	BACKGROUND.....	- 41 -
4.2	DEVELOPMENT.....	- 42 -
4.3	RESULTS	- 43 -
5.0	DESIGN OF MORTISE AND TENON JOINTS.....	- 46 -
5.1	INTRODUCTION	- 46 -
5.2	SELECTION OF A FACTOR OF SAFETY	- 46 -
5.3	LOAD DURATION FACTOR.....	- 49 -
5.4	DESIGN EQUATION.....	- 51 -
6.0	UTILIZATION OF YELLOW POPLAR.....	- 52 -
6.1	GENERAL INFORMATION	- 52 -
6.2	AVAILABILITY	- 53 -
6.3	MATERIAL PROPERTIES.....	- 53 -
6.3.1	<i>Strength</i>	- 53 -
6.3.2	<i>Drying</i>	- 54 -
6.3.3	<i>Workability</i>	- 55 -
6.4	CONCLUSION ON USAGE	- 55 -
7.0	SUMMARY AND CONCLUSIONS.....	- 56 -
7.1	JOINT RESEARCH.....	- 56 -
7.1.1	<i>Physical Testing</i>	- 56 -
7.1.2	<i>Finite Element Modeling</i>	- 57 -
7.2	DESIGN EQUATIONS AND CORRELATION.....	- 57 -
7.3	USAGE OF YELLOW POPLAR	- 58 -
7.4	RECOMMENDATIONS FOR FUTURE RESEARCH	- 58 -
8.0	REFERENCES.....	- 59 -
9.0	APPENDICES	- 61 -
	APPENDIX A – TENSION LOAD-DEFLECTION PLOTS.....	- 61 -

APPENDIX B – SHEAR LOAD DEFLECTION PLOTS..... - 68 -
APPENDIX C – DIRECT BEARING LOAD-DEFLECTION PLOTS..... - 72 -
APPENDIX D – DOWEL BEARING TEST DATA..... - 73 -
APPENDIX E – STATISTICAL METHODS FOR CORRELATION..... - 75 -

LIST OF FIGURES

FIGURE 1-1 - MORTISE AND TENON JOINT	- 3 -
FIGURE 1-2 - NDS DOUBLE SHEAR FAILURE MODES	- 3 -
FIGURE 2-1 - TENSION LOADING OF MORTISE AND TENON JOINT	- 9 -
FIGURE 2-2 - TENSION TESTING APPARATUS FROM SCHMIDT AND MACKEY (1997)	- 10 -
FIGURE 2-3 - JOINT DETAILING	- 11 -
FIGURE 2-4 - (A) MORTISE SPLITTING FAILURE (B) TENON RELISH FAILURE	- 13 -
FIGURE 2-5 - (A) PEG BENDING AND (B) SHEAR FAILURES	- 13 -
FIGURE 2-6 - FIVE PERCENT OFFSET YIELD	- 14 -
FIGURE 2-7 - YELLOW POPLAR CYCLIC TEST PLOTS	- 17 -
FIGURE 2-8 - (A) HOUSED JOINT COMMONLY FOUND IN PRACTICE FOR CARRYING SHEAR LOADS	- 19 -
FIGURE 2-9 - SHEAR TESTING APPARATUS	- 20 -
FIGURE 2-10 - TENON SPLITTING FAILURE DURING SHEAR LOADING	- 21 -
FIGURE 2-11 - ROLLING SHEAR FAILURE OF TENON IN SHEAR LOADING	- 22 -
FIGURE 2-12 - DOWEL BEARING FIXTURE WITH LOADING PERPENDICULAR AND PARALLEL TO GRAIN	- 26 -
FIGURE 3-1 - FINITE ELEMENT MODEL GEOMETRY FOR A MORTISE AND TENON JOINT	- 28 -
FIGURE 3-2 - STRESS - STRAIN CURVES USED IN FINITE ELEMENT MODELING	- 30 -
FIGURE 3-3 - MESHING OF MORTISE AND TENON JOINT	- 31 -
FIGURE 3-4 - 20-NODE BRICK ELEMENT (ANSYS, 2003)	- 33 -
FIGURE 3-5 - DETAIL OF CONTACT AND TARGET ELEMENTS NEAR PEG	- 33 -
FIGURE 3-6 - DISPLACED SHAPE OF THE JOINT	- 35 -
FIGURE 3-7 - SHORTLEAF PINE PHYSICAL AND MODELED LOAD-DEFLECTION CURVES	- 36 -
FIGURE 3-8 - RED OAK PHYSICAL AND MODELED LOAD-DEFLECTION CURVES	- 36 -
FIGURE 3-9 - EASTERN WHITE PINE PHYSICAL AND MODELED LOAD-DEFLECTION CURVES	- 37 -
FIGURE 3-10 - YELLOW POPLAR PHYSICAL AND MODELED LOAD-DEFLECTION CURVES	- 37 -
FIGURE 3-11 - DOUGLAS FIR PHYSICAL AND MODELED LOAD-DEFLECTION CURVES	- 38 -
FIGURE 3-12 - MESHING OF DIRECT BEARING MORTISE AND TENON JOINT	- 39 -
FIGURE 3-13 - EXPERIMENTAL AND MODELED DIRECT BEARING YELLOW POPLAR JOINTS	- 40 -
FIGURE 3-14 - MODELED DIRECT BEARING CURVES FOR VARIOUS SPECIES	- 40 -
FIGURE 4-1 - FOUR SHEAR PLANES USED IN CONVERTING YIELD LOAD TO YIELD STRESS	- 42 -
FIGURE 4-2 - PLOT OF YIELD POINTS WITH CORRELATION SURFACE	- 45 -
FIGURE 4-3 - CORRELATION SURFACE AND DATA POINTS VIEWED ALONG EDGE	- 45 -
FIGURE 5-1 - MADISON CURVE SHOWING LOAD DURATION FACTORS	- 50 -
FIGURE 6-1 - NATURAL RANGE OF YELLOW POPLAR (FS-272)	- 52 -

LIST OF TABLES

TABLE 2-1 - RESULTS OF YELLOW POPLAR TENSION TESTING	- 15 -
TABLE 2-2 - RESULTS OF CYCLIC TESTING OF YELLOW POPLAR	- 16 -
TABLE 2-3 - MINIMUM DETAILING REQUIREMENTS AS A MULTIPLIER OF THE PEG DIAMETER (D)	- 18 -
TABLE 2-4 - RESULTS OF YELLOW POPLAR SHEAR TESTING	- 23 -
TABLE 2-5 - RESULTS OF YELLOW POPLAR DIRECT BEARING TESTS	- 24 -
TABLE 3-1 - MATERIAL PROPERTIES FROM THE WOOD HANDBOOK	- 29 -
TABLE 3-2 - RESULTS OF MESH REFINEMENT STUDY USING ORTHOTROPIC YELLOW POPLAR PROPERTIES AND SUBJECTED TO 3500 POUNDS OF LOAD	- 32 -
TABLE 3-3 - COMPARISON OF PHYSICAL AND MODELED JOINTS	- 35 -
TABLE 4-1 - SPECIFIC GRAVITY AND YIELD STRESS DATA USED IN DEVELOPING THE CORRELATION	- 44 -
TABLE 5-1 - RATIO OF YIELD LOAD TO ULTIMATE LOAD FOR FULL-SIZED JOINTS	- 47 -
TABLE 5-2 - RATIO OF CORRELATION STRENGTH TO EYM MODE IIIS ALLOWABLE LOAD	- 48 -
TABLE 5-3 - EXAMPLE ON THE PROPER USAGE OF THE CORRELATION	- 51 -
TABLE 6-1 - DIMENSIONAL CHANGE IN 3" LUMBER (IN INCHES) (FOREST PRODUCTS LAB, 2000)	- 54 -

LIST OF EQUATIONS

EQUATION 4-1	- 42 -
EQUATION 4-2	- 43 -
EQUATION 5-1	- 51 -

1.0 Introduction

1.1 History and Background

Timber framing consists of large, widely spaced timbers connected together with all-wood connections, such as mortises, tenons and pegs. It is one of the most traditional forms of construction, having been practiced since before Christ (Benson and Gruber, 1980). As the quality of tools improved, timber framing expanded to its peak in the 17th century in Europe. As the United States was settled and timber was plentiful, groups of immigrants brought their own style of timber framing from the old country (Sobon and Schroeder, 1984). This influx of styles, combined with the availability of tall, large diameter trees, allowed for the United States to create its own strong and rich timber-framing tradition.

With the advent of the industrial revolution, during which commercial sawmills developed the capacity to mass produce small pieces of lumber, balloon framing methods developed. In this building style, long pieces of dimensional lumber ran from the sill to the eave. Currently, platform framing is the most common method for wood frame construction, in which vertical lumber spans only from floor to floor. The advent of these other building methods caused timber framing, which required ever harder-to-find large timbers and skilled labor, to nearly fade into history

In the early 1970s, there was a strong interest in reviving lost folk crafts in the United States; among them was timber-framing. Early in the revival, the skills needed to construct a frame were developed by examination of old timber frames and by trial and error, for there were no longer any experienced craftsman to pass along the trade. Today,

timber framing has grown from the craft revival days of three decades past into a strong, although niche, industry.

1.2 Problem Statement

Standard mortise and tenon joints (Figure 1-1) can adequately carry shear and compressive forces from the beam into the post through direct bearing of wood against wood. Under wind and other loading situations, a joint may experience tensile forces that attempt to pull the tenon out of the mortise. In this situation, the connection forces must be transferred between the mortise and tenon through wooden pegs. Pegs are wooden pins, while the term dowel usually refers to a steel pin.

Current procedures included in the National Design Specification (NDS) for Wood Construction (AFPA, 2001) specify methods for designing joints in which the dowel connector is steel, not wood. These procedures are based on the European Yield Model (EYM) which describe failure modes of dowel connected wood joints. Figure 1-2 shows the standard double shear failure modes. Modes I_m and I_s are dowel bearing failures of the base material. Mode III_s , which is similar to the failure mode commonly observed in pegged timber joints, occurs when the dowel develops one or two flexural hinges in the main member while crushing the base material. Mode IV occurs when two flexural hinges form in the dowel connector for each shear plane. The smallest predicted load from these failure modes is the value used in design.

The EYM failure modes are based on steel dowel connectors, not wooden pegs. Hence, designers of timber frames have little guidance when designing wood based

joinery for load transfer. They require a design method for mortise and tenon joints loaded in tension that can be incorporated into the NDS.

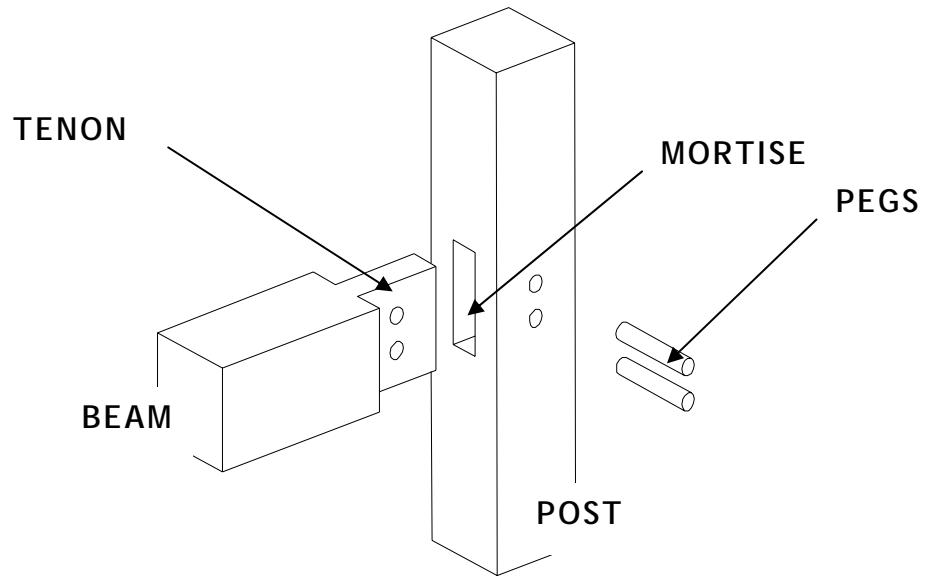


Figure 1-1 - Mortise and Tenon Joint

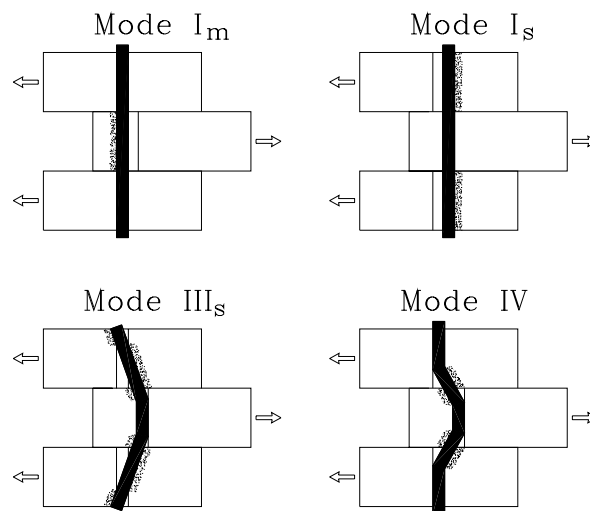


Figure 1-2 - NDS Double Shear Failure Modes

1.3 Literature Review

Research pertaining to timber framing, in general or in specifics, is very limited, with most research having been conducted only in the last few years. The all-wood connections employed in timber-framing render the research conducted on bolted post and beam construction useful for only comparison's sake.

Despite long traditions of using timber-frame structures in Europe, little applicable research has been found, with the exception of research by Kessel and Augustin in Germany (Kessel & Augustin, 1995) (Kessel & Augustin, 1996). Their work focused on the tensile load capacity for mortise and tenon joints and appropriate design values.

The first notable research conducted in the United States on timber frames was by Brungraber, in which the frame behavior was studied with only limited review of individual joint tests (Brungraber, 1985).

More recently, research conducted at the Michigan Technological University by Reid included experimental studies of mortise and tenon joinery (Reid, 1997). These tests were conducted on full-sized connections mocked up from dimension lumber. Reid correlated experimental results to predictions from the European Yield Model (EYM) equations for double shear connections, the current NDS standard. EYM Mode III_s predicted the yield load of the mortise and tenon joints quite well. Failure modes in the experimental specimens were similar to common failure modes witnessed in full-sized mortise and tenon connections.

Drewek, also of the Michigan Technological University, conducted research based on the modeling of a traditional timber frame bents. Strength parameters for the individual joints were developed analytically, not experimentally (Drewek, 1997).

At the University of Wyoming, MacKay focused on modification of the EYM failure modes to more accurately predict connections with wooden dowels (Schmidt and MacKay, 1997). With the addition of various yield modes, the EYM could be used to design pegged connections. Tests were also conducted to determine the mechanical properties of the pegs commonly associated with mortise and tenon joinery. These tests included dowel bearing, shear, and bending strengths of pegs.

Following MacKay's work, Daniels conducted research on full-sized traditional mortise and tenon joints (Schmidt and Daniels, 1999). This work included development of detailing requirements, such as end and edge distances, to ensure a ductile peg failure. Mechanical properties of the various materials, including dowel bearing, peg bending, and peg shear strength were conducted. A method to relate the diameter of a peg to the diameter of an equal-strength steel bolt was also developed. This allows for the direct usage of the EYM equations for pegged joints.

Scholl, also of the University of Wyoming, expanded on previous work by showing that draw-boring increases joint stiffness but does not alter a joint's yield capacity (Schmidt and Scholl, 2000). Most timber-framed buildings are constructed from green timbers and loaded to at least partial capacity for extended amounts of time. Scholl also explored seasoning and load-duration effects on full-sized joints. These tests resulted in the modification of the detailing requirements developed by Daniels.

Erikson conducted research on single- and multiple-story bents subjected to lateral load (Erikson, 2003). Bents covered with stress-skin panels were also tested, and frame stiffness parameters were developed. No work was performed to isolate behavior of the individual joints.

Although most finite element modeling of dowel-connected wooden joints had focused on the use of a steel dowel, by changing material properties, the research becomes applicable to wooden pegged mortise and tenon joints. Patton-Mallory and her colleagues studied nonlinear material models for bolted connections and developed a tri-linear stress-strain constitutive model for the wood behavior (Patton-Mallory et al., 1997). They developed a three-dimensional model of a bolted wooden connection that closely followed experimental load deflection curves.

Kharouf, McClure, and Smith also developed an elasto-plastic model for bolted wood connections loaded in both tension and compression. They derived their constitutive model from mechanics of materials theories and included anisotropic hardening. When compared to experimental results, the numerical model slightly over predicted the stiffness of the joint (Kharouf et al., 2003).

Chen, Lee, and Jeng also explored timber joints with dowel-type fasteners using the finite element method. They used Hooke's law to describe the stress-strain relationship for both normal and fiberglass reinforced joints with a metal dowel fastener. Experimental results compared fairly well with the models (Chen et al., 2003).

1.4 Objectives and Scope of Work

The primary goal of this research is to develop a design method for pegged mortise and tenon joints loaded in tension. An accepted design method will give engineers and designers more confidence in using mortise and tenon joints in tension. The design method developed here is based on a correlation between the specific gravities of the wood and the allowable shear stress in the pegs. The correlation is developed with data from new and previously conducted physical testing of joints, as well as with data from finite element analyses. The completed design method allows for the determination of the load capacity of a pegged joint, whether or not physical or numerical testing has been conducted on that combination of peg and base material.

The secondary goal of this research is to continue previous work conducted at the University of Wyoming in developing minimum detailing requirements for pegged mortise and tenon joints. Specifically, detailing requirements for yellow poplar were developed. This included determining the suitability of yellow poplar as a timber framing material. Yellow poplar is an eastern hardwood that is fast growing, straight, easy to work, and economical. Yet yellow poplar has not been used as a timber framing material in recent times. By conducting physical testing on yellow poplar mortise and tenon joints, a comparison can be made to other common species, and possibly confidence can be instilled in using this plentiful and underutilized resource.

2.0 Testing Procedures and Results

Testing consisted of four different types of tests. The first and most extensive tests were conducted on mortise and tenon joints with the tenon loaded in tension. Tests were also conducted on the shear loading of a tenon where the load was transferred through the pegs. Joints were also tested in shear where the tenon beared directly in the mortise. Dowel bearing tests, used to determine the dowel bearing strength of wood, were also conducted.

Moisture content and specific gravity tests were conducted on each of the test specimens used in all of the physical testing, including tensile, shear, direct tenon bearing, and dowel bearing tests. The moisture content testing was conducted following ASTM D4442. Samples were cut from the specimens immediately following testing, weighed, measured and oven-dried for 24 hours. Specific gravity tests, following ASTM D2395, were conducted with the same samples as in the moisture content test.

2.1 Joint Tests

2.1.1 Tension Testing

2.1.1.1 Introduction

Full-sized joints were tested to determine the strength and stiffness of mortise and tenon joints tested in tension and shear. The species *Liriodendron tulipifera*, commonly known as yellow or tulip poplar, was used for the base material for two main reasons. First, its specific gravity fills in a gap in data collected previously at the University of Wyoming. This additional data helped in development of a correlation between the

specific gravity of the joint material, that of the pegs, and the strength of a joint. Secondly, the feasibility of using yellow poplar in timber framed structures was explored because of its historical usage in covered bridges and its availability in the eastern and midwestern United States.

Tension testing consisted of applying a tension force to a tenoned member to withdraw it from its connection to a mortised member. The connection was secured with wooden pegs (Figure 2-1). This type of loading can be developed in a timber-framed structure during lateral loading.

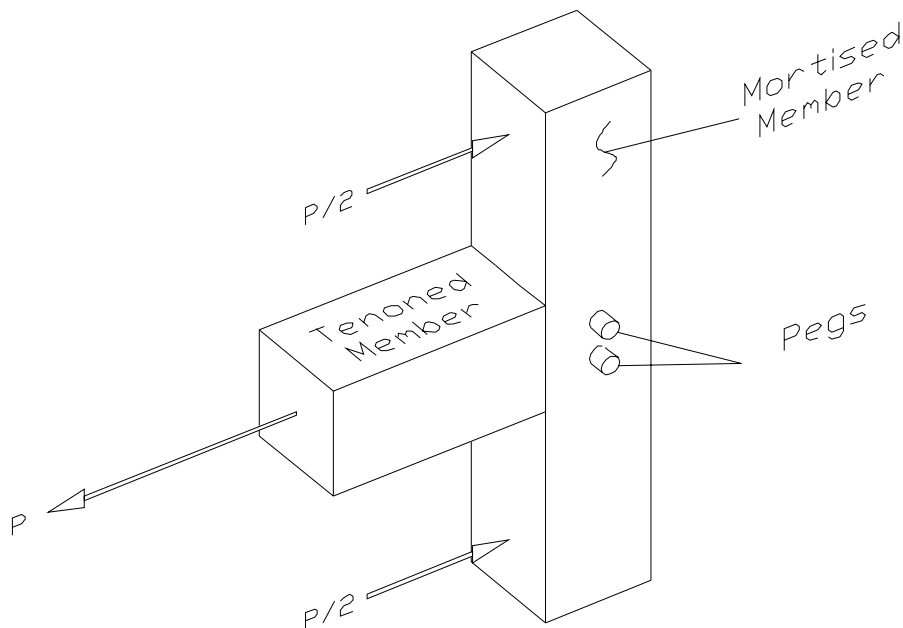


Figure 2-1 - Tension Loading of Mortise and Tenon Joint

2.1.1.2 Procedure

Tension testing on full-sized mortise and tenon joints was conducted using a steel load frame (Figure 2-2) and an Enerpac RCH 123 hydraulic ram operated by a hand

pump. Two string potentiometers, one on each side of the joint, measured relative deflection of the mortised and tenoned members thereby discounting any deflection in the frame. The measurements were averaged to provide a single joint deflection measurement, which was then recorded by Labview data acquisition software. A 2000 psi pressure transducer was used to record the pressure in the system, which was then correlated through the area of the hydraulic ram to the load on the joint.

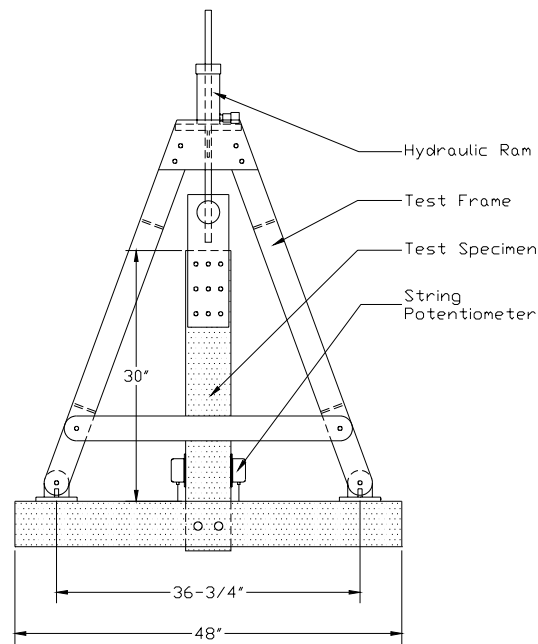


Figure 2-2 - Tension Testing Apparatus from Schmidt and MacKay (1997)

Mortise and tenon joints were cut to common construction tolerances at the University of Wyoming with standard timber-framing tools. The moisture content of the yellow poplar ranged from 20% to 63% during testing, and each joint was tested immediately after cutting. No attempt was made to equilibrate the timbers to a particular moisture content. Obvious defects such as checks and knots were avoided in the joint

area whenever possible. Varying species of pegs, including red oak, white oak, sugar maple, white ash, and paper birch, were used. All pegs were nominally one inch in diameter and at an average moisture content of 6.8%.

The tenon thickness was varied between tests from 1.5 to 2 inches, the common tenon thicknesses for hardwoods and softwoods, respectively. This was to help determine if yellow poplar, being a relatively soft hardwood, behaved more like a hardwood or like a softwood.

In addition to strength and stiffness data for the yellow poplar joints, detailing requirements were also developed to ensure that peg failure preceded member failure. End (l_e), edge (l_v), and spacing (l_s) distances were varied accordingly (Figure 2-3). Pegs fail in a somewhat ductile manner, whereas failure of the tenon relish or the mortise cheeks occurs in a sudden and brittle fashion. By ensuring peg failures, a joint can be repaired after an extreme loading event by replacing the damaged pegs. Joints were tested with excessive end, edge, and spacing distances to ensure peg failure in the joints tested first. The detailing was then modified in subsequent tests until relish and mortise cheek failures occurred, and then backed off for the minimum detailing requirements.

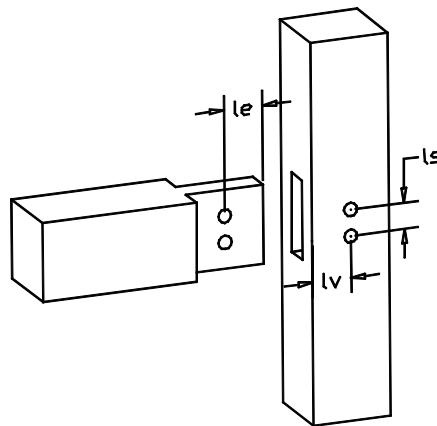


Figure 2-3 - Joint Detailing

Load was applied to the joints at a uniform stroke rate in an attempt to reach failure in 10 minutes. After failure, the joint was disassembled and inspected to determine the mode of failure. Several joints were retested using different species of pegs if there was little or no visible dowel bearing failure in the timbers.

Two joints were loaded cyclically to obtain hysteresis data. The joints were loaded and unloaded in increasing increments of 0.05 inches until failure. Failure was determined as when the joint would no longer take on any more load.

2.1.1.3 Joint Failures

Of the twenty-two tests performed on eighteen different yellow poplar joints, four failure modes were observed during the testing, two in the timber material, two in the peg. The first timber failure was splitting of the mortised member due to tension perpendicular to the grain. The load-limiting split started from the peg hole and propagated outward (Figure 2-4a). The split usually occurred suddenly and audibly, and continued to grow as the joint was deflected farther. This failure occurred because of inadequate edge distance on the mortised member.

The other timber failure is known as a relish failure and can either be a single split, which develops on the end of the tenon behind the peg hole, or a block rupture failure of the material behind the peg hole (Figure 2-4b). The splitting failure was load limiting but allowed the joint to hold the failure load. Dual block rupture failures resulted in loss of load capacity in the joint. Both of these failures, which can occur behind one or both of the pegs or in combination, are caused from inadequate end distance on the tenon.

The ductile peg failures were either of a bending type, where a flexural hinge developed in the peg at the center of the tenon (Figure 2-5a), or of a shearing type, where the peg sheared at the two interface planes between the mortise and tenon (Figure 2-5b). In the yellow poplar joint tests, peg bending failures were much more common than the shearing type. This behavior can be attributed to the low dowel bearing strength of the yellow poplar timber versus the oak pegs. The low dowel bearing strength allowed the peg hole in the mortise and tenon to crush. Previous research has shown that pegged joints in timber with high dowel bearing strength are more likely to fail by peg shear (Daniels, 1999). A combination of shearing and bending failures occurred in most of the joints, with the most noticeable portion of the damage to the peg caused by bending.

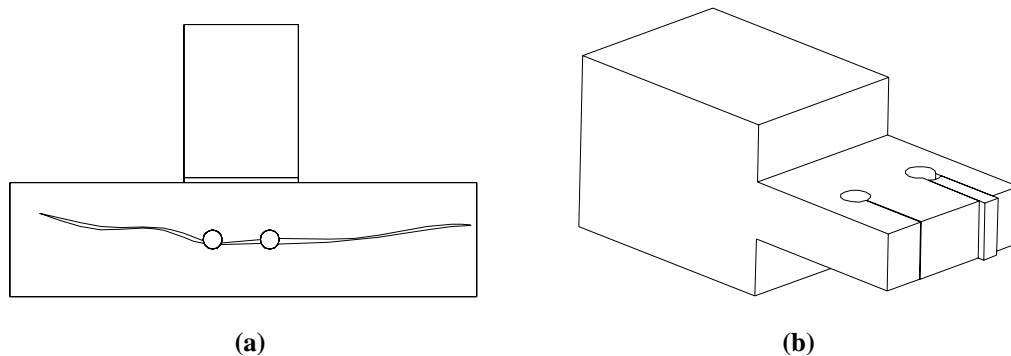


Figure 2-4 - (a) Mortise Splitting Failure (b) Tenon Relish Failure

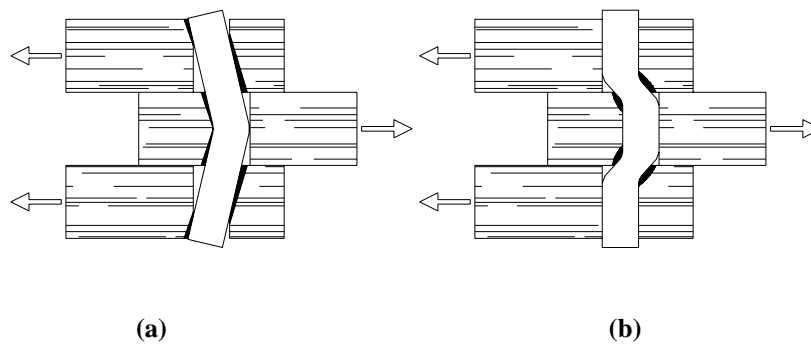


Figure 2-5 - (a) Peg Bending and (b) Shear Failures

2.1.1.4 5% Offset Analysis

Following ASTM D5652 and ASTM D5764, which are for bolted wood connections, a 5% offset yield method was used in determining the yield load for each of the joint tests. To determine the yield load, the initial linear portion of the load-deflection curve is identified, and then a line with the same slope as the initial linear portion is offset along the deflection axis 5% of the dowel-connector diameter. The point where this offset line intercepts the load deflection curve is defined as the yield point. If the offset line does not intersect the load deflection curve, then the maximum load the joint reaches is taken as the yield load. Figure 2-6 depicts a load-deflection plot with the 5% offset yield value.

Due to the nature of load-deflection plots for mortise and tenon joints, choosing the initial linear portion of the curve is somewhat subjective. To limit the variability in choosing the initial linear portion, the two data points chosen to describe the line were taken as far apart on the curve as possible. A line was then plotted between these two points to ensure that it did in fact describe the linear portion of the plot.

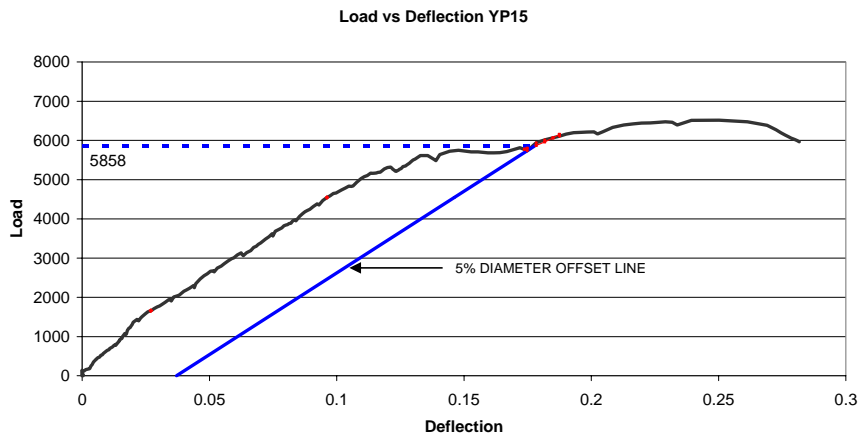


Figure 2-6 - Five Percent Offset Yield

2.1.1.5 Results

Eighteen yellow poplar joints were subjected to twenty two tension tests; twenty loaded monotonically and two cyclically to failure. The mean yield load for the joints was 5,549 pounds at a deflection of 0.138 inches. Table 2-1 includes the results of the monotonic tensile testing. The detailing of the peg locations is included as a function of the peg diameter *D*. One-inch diameter pegs were used exclusively for these tests. The reported stiffness is the slope of the five percent offset line, which corresponds to the initial straight line portion of the load deflection plot. Varying the tenon thickness did not seem to have any noticeable effect on the strength or stiffness of the joint. Individual test load-deflection plots can be found in Appendix A.

Table 2-1 - Results of Yellow Poplar Tension Testing

		Peg Species	le	lv	ls	Yield Disp. in	Yield Load lb	Yield Stress psi	Stiffness lb/in	Ult. Disp in	Ult. Load lb	Base G	Avg MC %	Peg G	Peg MC %	Failure at Yield	Failure at Ultimate
2" Thick Tenon	YP 1	R. OAK	3.0	3.0	3.0	0.140	6,970	2,220	53,300	0.833	7,880	0.41	44%	0.65	7.4%	Peg	Peg & Mortise
	YP 2	R. OAK	1.8	3.0	2.5	0.092	4,480	1,430	100,900	0.187	5,970	0.43	57%	0.56	6.5%	Peg	Relish
	YP 3	W. OAK	2.5	3.5	3.0	0.203	6,460	2,060	34,700	0.203	6,460	0.47	55%	0.69	8.8%	Peg	Peg
	YP 4	W. OAK	1.5	3.5	3.0	0.121	5,790	1,840	73,000	0.164	6,030	0.47	59%	0.67	7.2%	Relish	Relish
	YP 5	W. OAK	2.0	3.0	3.0	0.140	4,510	1,440	33,200	0.955	6,890	0.45	47%	0.58	6.9%	Peg	Peg & Mortise
	YP 6	W. OAK	3.0	3.0	3.0	0.229	6,920	2,200	36,200	0.235	7,020	0.44	39%	0.86	5.3%	Peg	Peg
	YP 6b	MAPLE	3.0	3.0	3.0	0.222	6,620	2,110	38,700	0.230	6,680	0.44	39%	0.64	6.0%	Peg	Peg
	YP 6c	ASH	3.0	3.0	3.0	0.228	6,130	1,950	28,900	0.228	6,130	0.44	39%	0.60	6.2%	Peg	Peg
1.5" Thick Tenon	YP 6d	BIRCH	3.0	3.0	3.0	0.043	7,630	2,430	33,300	0.291	7,970	0.44	39%	0.66	6.9%	Peg	Peg
	YP 7	W. OAK	2.0	3.5	3.0	0.124	4,450	1,410	39,800	0.328	5,610	0.39	63%	0.73	8.5%	Peg	Peg
	YP 7b	BIRCH	2.0	3.5	3.0	0.173	4,740	1,510	35,000	0.948	6,000	0.39	63%	0.65	5.8%	Peg	Peg
	YP 8	W. OAK	2.0	3.0	3.0	0.078	6,260	1,990	164,700	0.145	7,100	0.41	58%	0.63	4.7%	Peg	Peg
	YP 10	W. OAK	3.0	3.0	3.0	0.084	6,000	1,910	96,400	0.710	7,620	0.42	48%	0.64	7.8%	Peg	Peg & Relish
	YP 11	W. OAK	2.0	2.0	3.0	0.037	5,110	1,630	43,300	0.215	6,250	0.50	38%	0.63	7.0%	Peg	Peg
	YP 12	W. OAK	1.5	1.5	2.0	0.105	4,050	1,290	47,900	0.148	4,220	0.42	38%	0.72	7.5%	Relish	Relish
	YP 13	W. OAK	2.0	1.5	1.5	0.114	3,370	1,070	47,900	0.284	5,770	0.44	32%	0.62	7.8%	Peg	Peg
	YP 14	W. OAK	1.5	1.5	1.5	0.176	4,800	1,530	33,300	0.204	5,190	0.49	42%	0.77	7.2%	Relish	Relish
YP 15	W. OAK	2.0	2.0	3.0	0.172	5,860	1,860	41,700	0.250	6,520	0.48	32%	0.68	5.9%	Peg	Peg	
YP 16	W. OAK	3.0	3.0	3.0	0.120	5,290	1,680	68,100	0.235	6,440	0.47	32%	0.64	6.5%	Peg	Peg	
YP 17	W. OAK	3.0	3.0	3.0	0.168	11,620	1,850	90,200	0.295	12,210	0.47	36%	0.68	6.8%	Peg	Peg & Relish	
							Mean	1713	62,790	*Excludes the repaired and cyclically loaded joints							
							St Dev	333	35,570								
							COV	19.5%	56.6%								

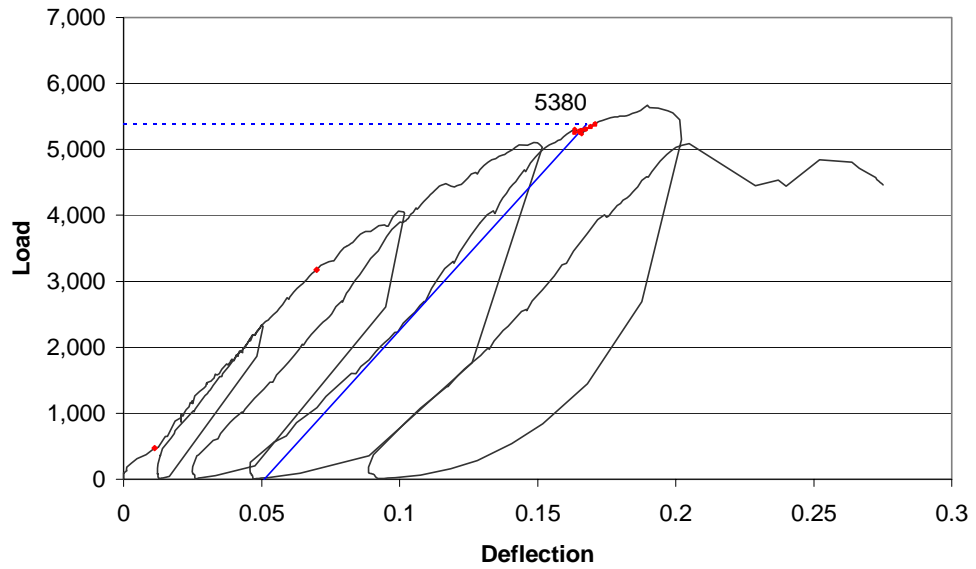
Previous research has shown that joints loaded cyclically perform in a similar fashion to monotonically loaded joints (Schmidt and Daniels, 1999). In this research, the cyclic hysteresis tests were conducted to determine if the pegged mortise and tenon joints in yellow poplar maintained their ductile behavior even with repeated loading. As each joint was loaded in a subsequent cycle, the envelope of the load-deflection curve closely matched that of the monotonic tension tests loaded to failure in a single cycle (Figure 2-7). This suggests there is enough toughness in these timber joints to withstand repeated loading cycles. The mean yield load for two cyclically loaded joints was 5,940 pounds; slightly higher than the monotonically loaded joints. Other pertinent results of the hysteresis tests are included in Table 2-2.

Both of the cyclically loaded joints had white oak pegs. The 2.0 inch thick tenon had 3.5 inches of relish, while the pegs were spaced 2.0 inches apart and placed 2.0 inches from the edge of the mortise.

Table 2-2 - Results of Cyclic Testing of Yellow Poplar

	Yield Disp. in	Yield Load lb	Yield Stress psi	Stiffness lb/in	Ult. Disp in	Ult. Load lb	Base G	Avg MC %	Peg G	Peg MC %	Failure at Yield	Failure at Ultimate
H1	0.163	5,380	1,710	46,100	0.190	5,670	0.461	6.1%	0.64	6.6%	Peg	Peg
H2	0.130	6,500	2,070	65,100	0.133	6,590	0.492	11.2%	0.71	7.2%	Peg	Peg
Mean		1,890	55,600									
St. Dev		255	13435									
COV		13.5%	24.2%									

Load vs Deflection YPH1



Load vs Deflection YPH2

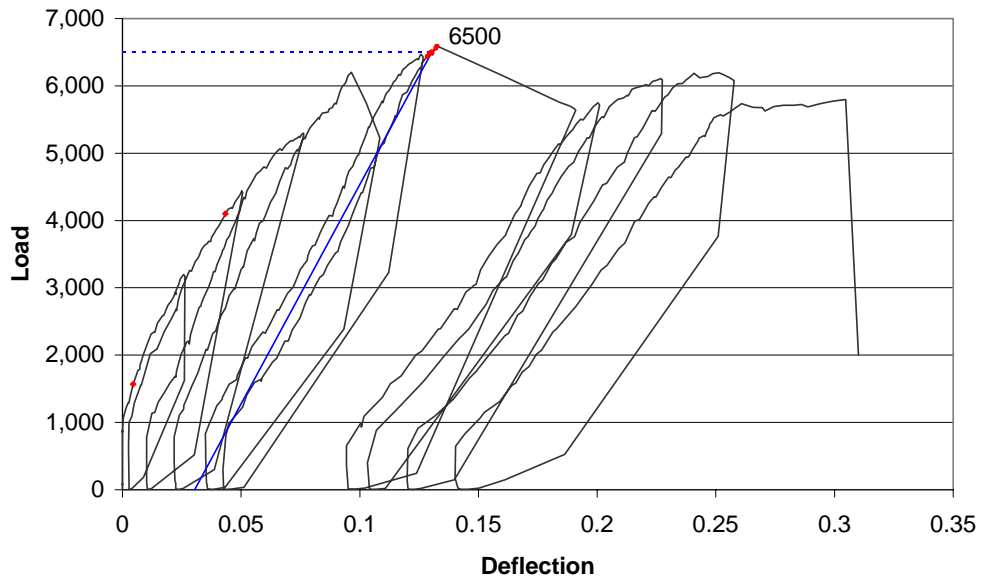


Figure 2-7 - Yellow Poplar Cyclic Test Plots

2.1.1.6 Detailing Requirements

Detailing requirements that ensure a peg failure at both yield and ultimate load levels were developed for design purposes. These detailing requirements are based on short-term loading of unseasoned joints. Load duration, seasoning and drawboring effects required that the detailing requirements be increased by 0.5 D (Schmidt & Scholl, 2000). Also, relatively few tests were conducted with other than one-inch diameter pegs. This limits the detailing requirements to use with only one inch-diameter pegs. Table 2-3 includes minimum detailing requirements based on the yield condition taken from Schmidt and Scholl (2000) along with new yellow poplar data.

Table 2-3 - Minimum Detailing Requirements as a Multiplier of the Peg Diameter (D)

	End le (D)	Edge lv (D)	Spacing ls (D)
Douglas Fir	2	2.5	2.5
Eastern White Pine	4	4	3
Red & White Oak	2	2	2.5
Southern Yellow Pine	2	2	3
Yellow Poplar	2.5	2.5	3

2.1.2 Shear Testing

2.1.2.1 Introduction

Shear testing consisted of loading a tenoned member, again pegged into a mortise, in shear. This loading situation could occur anywhere that the tenoned member carries gravity loads. The geometry of these joints varied from what would be found in practice. Normally the bottom of the tenoned member rests along its full width in a housing in the

mortised member (Figure 2-8a). For this joint configuration, shear load is transferred through direct bearing between the two members. The pegs only serve to secure the joint during construction and to resist tension loading. For the tests, an oversized mortise was cut to ensure that no bearing contact occurred between the mortise and tenon (Figure 2-8b). Rather, all of the load was transferred through the peg.

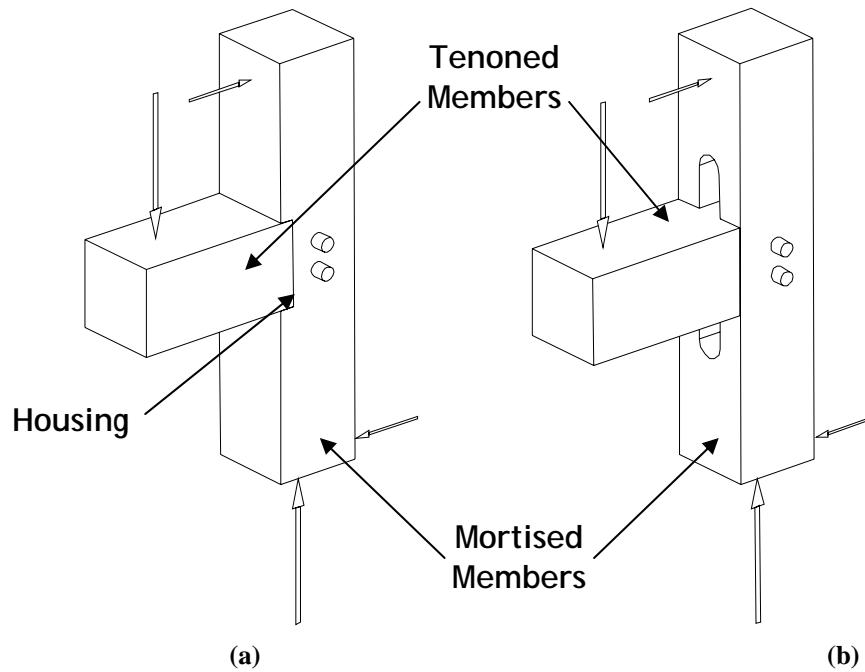


**Figure 2-8 - (a) Housed Joint Commonly Found in Practice for Carrying Shear Loads
(b) Open Mortise Joint Used In Shear Loading Testing**

2.1.2.2 Procedure

Shear testing on full-sized mortise and tenon joints was conducted using a steel load frame (Figure 2-9) and an Enerpac RCH 302 hydraulic ram operated by a hand pump. Two string potentiometers, one on each side of the joint, measured deflection of the joint. The measurements from the two string pots were averaged to find a mean joint deflection. Pressure from a 5000 psi pressure transducer and deflections from the string pots were recorded using Labview data acquisition software.

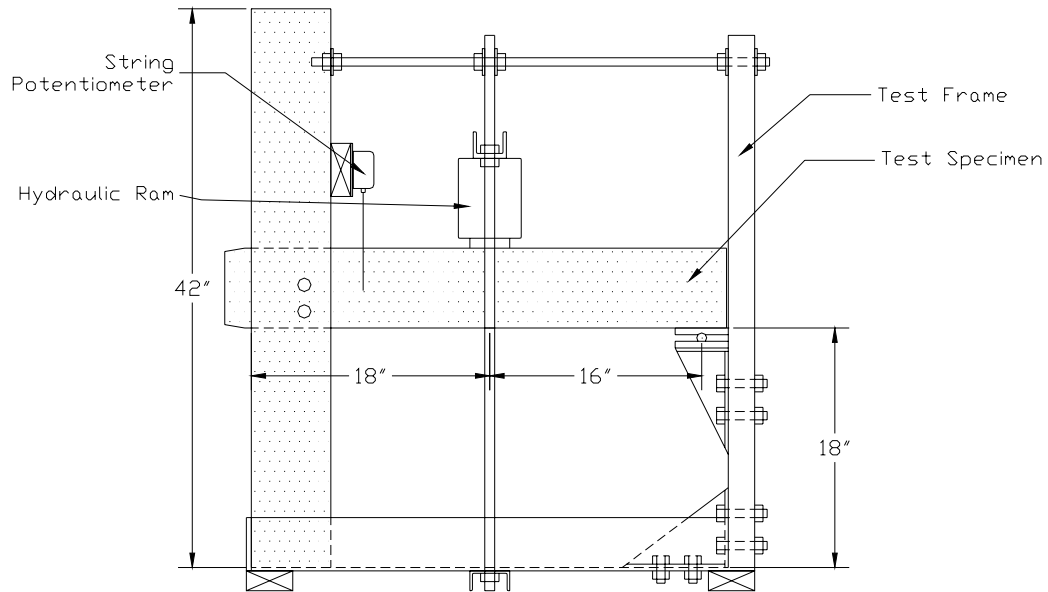


Figure 2-9 - Shear Testing Apparatus

Mortise and tenon joints were cut at the University of Wyoming with two major differences compared to the tension joints. In order to eliminate the possibility of a tenon bearing in the bottom of a mortise during shear loading, there was extra relief cut into the mortise to allow for nearly unlimited tenon deflection (Figure 2-8). Also, two-inch thick tenons were used exclusively to keep the longitudinal net section of the tenon as large as possible. The moisture content of the yellow poplar ranged from 20 to 40 percent, while the equilibrated pegs averaged 6.3 percent.

Testing was conducted using various lengths of tenons, number of pegs, and location of the peg holes. Load was applied to the joints through the hydraulic ram at a constant stroke rate to induce failure in about 10 minutes. After the joint failed, the pieces were disassembled and inspected to determine the mode of failure. Failure was defined as the condition at which the joint would no longer take on any more load. Two

joints were retested using different species of pegs when inspection showed only peg failures. Moisture content and specific gravity tests were then performed on specimens taken from each member.

2.1.2.3 Joint Failures

Twelve tests were performed on eight different joints; only two distinct failure modes occurred. The most common and least desirable failure mode was tenon splitting due to tension perpendicular to grain, always through the bottom peg hole (Figure 2-10). A few rolling shear failures also occurred in combination with the tenon splitting failures (Figure 2-11). Tenon splitting failures occurred even when only one peg was used.

In a few instances in which long through tenons were used, pegs failed in the same bending fashion as occurred in the tension testing. There were no shear failures of the pegs, possibly due to the low dowel bearing strength perpendicular to grain in the tenon.

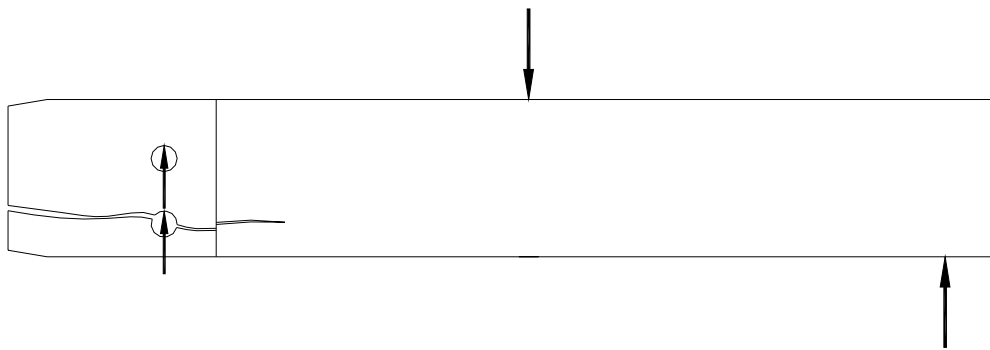


Figure 2-10 – Tenon Splitting Failure During Shear Loading

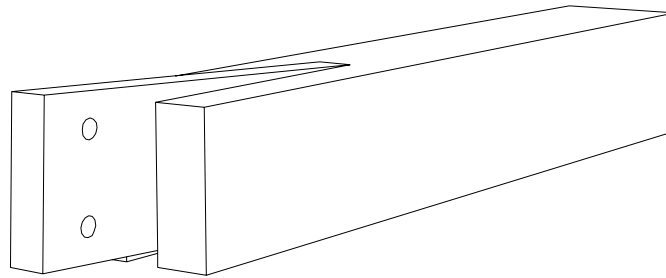


Figure 2-11 - Rolling Shear Failure of Tenon in Shear Loading

2.1.2.4 Results

Five-percent offset yield load analyses were conducted on each of the tests following the method outlined in the tension testing. This yield data is listed in Table 2-4 along with the joint detailing and failure modes. Load-deflection plots can be found in Appendix B. The extremely long tenons required to achieve pure peg failures made it impractical to recommend detailing requirements for these joints. Placing the pegs lower in the tenon did help increase the strength of the joint. However, the small sample size made it difficult for a conclusive relation to be drawn. Based on these tests though, it is clear that shear loads are more appropriately carried through direct bearing in housed joints (Figure 2-8a) than by load transfer through pegs.

Table 2-4 - Results of Yellow Poplar Shear Testing

		Species	le	lv	ls	Yield Disp.	Yield Load	Yield Stress	Stiffness	Ult. Disp	Ult. Load	Base G	Avg MC	Peg G	Peg MC	Failure at Yield	Failure at Ultimate
			D	D	D	in	lb	psi	lb/in	in	lb		%	%			
YP	S1	W. OAK	5	3	3	0.144	2,700	860	27500	0.494	5,260	0.50	30%	0.68	6.2%	Tenon	Tenon
YP	S2	W. OAK	6	2	2.5	0.204	5,880	1,870	37,500	0.715	6,950	0.48	35%	0.73	6.2%	Tenon	Peg
YP	S3	W. OAK	7	1.5	1.5	0.190	5,240	1,670	32,800	0.398	7,690	0.46	40%	0.68	8.3%	Beam	Beam
YP	S4	W. OAK	6	1.5	1.5	0.186	5,460	1,740	30,500	0.186	5,460	0.46	26%	0.63	5.6%	Peg	Peg
YP	S4B	MAPLE	6	1.5	1.5	0.243	6,190	1,970	26,600	0.243	6,190	0.46	26%	0.64	7.5%	Peg	Peg
YP	S4C	BIRCH	6	1.5	1.5	0.216	5,610	1,780	27,000	0.349	6,620	0.46	26%	0.62	7.3%	Peg	Peg
YP	S5	W. OAK	6.5	1.5	1.5	0.188	5,800	1,850	39,600	0.212	6,100	0.47	23%	0.64	4.0%	Peg	Peg
YP	S6	W. OAK	3.5	1.5	1.5	0.142	2,850	910	29,800	0.444	4,490	0.46	27%	0.71	6.3%	Tenon	Tenon
YP	S7	W. OAK	4.5	1.5	N/A	0.196	3,510	1,120	23,400	0.380	4,880	0.46	27%	0.72	10%	Tenon	Peg
YP	S7B	W. OAK	4.5	1.5	N/A	0.443	5,420	1,730	13,400	0.543	5,850	0.46	27%	0.81	8.6%	Tenon	Peg
YP	S7C	STEEL	4.5	1.5	N/A	0.525	6,440	2,050	12,600	0.926	8,180	0.46	27%	7.84	0.0%	Tenon	Tenon
YP	S8	W. OAK	6	1.5	1.5	0.203	5,170	1,650	32,700	0.830	7,520	0.46	27%	0.72	5.1%	Tenon	Peg

Average	1460	31,730	* Excludes the repaired and steel dowel joints
St. Dev	424	5,210	
COV	29.0%	16.4%	

2.1.3 Direct Bearing Tests

Upon the conclusion of shear testing of the mortise and tenon joints, two more tests were conducted using the same setup. These tests were used to determine the joint stiffness and capacity in shear if the tenon were allowed to bear directly on the bottom of the mortise. Both joints failed with some rolling shear effects.

Testing of the shear joints in direct bearing was performed without the use of pegs. The greater stiffness of the tenon bearing in the mortise would establish the preferred load path, thus limiting the amount of shear load the pegs would carry if included. Special effort was made to cut the bottom of the mortises as flat as possible to ensure uniform bearing of the tenon. Testing was conducted in a fashion similar to the previous shear testing. A joint was deemed “failed” when it exceeded a deflection allowable in service. A summary of the pertinent test results is included in Table 2-5. Load deflection plots of the two joints are also included in Appendix C.

The result of these tests showed that direct bearing of the tenon in the mortise provides for a considerably stiffer and stronger joint. The compressive strength perpendicular to the grain of the tenon seemed to be a limiting factor on the joint stiffness.

Table 2-5 - Results of Yellow Poplar Direct Bearing Tests

	Yield Disp.	Yield Load	Stiffness	Ult. Disp	Ult. Load	Base G	Avg MC
	in	lb	lb/in	in	lb		%
B1	0.21	9,240	61,530	0.45	11,660	0.448	22.8%
B2	0.26	9,570	44,010	0.70	15,420	0.474	10.5%
		Mean	52,770				
		St. Dev	12,390				
		COV	23.5%				

As a tenon becomes heavily loaded in shear, there is a tendency for a rolling shear failure to occur (Figure 2-11). This failure happens suddenly and causes the member to lose load-carrying capacity. Rolling shear is a failure commonly found in plywood and other sheet materials acting in diaphragms. In solid wood, it can occur in tenoned members but is highly variable due to the complex geometry over which the shearing action occurs.

During testing of the pegged shear joints and the direct bearing shear joints, rolling shear failures occurred as the ultimate mode of failure in some of the tests. Due to the immeasurable area over which the rolling shear occurred, it is difficult to quantify the capacity of wood in rolling shear. The Wood Handbook (1999) reports that the rolling shear capacity is the range of 18 to 28 percent of the parallel to grain shear values. Therefore, tenons should not be relied on for shear load transfer because of the brittle

failure mode. Rather, shear transfer is better achieved through housed joints (Figure 2-8a).

2.2 Dowel Bearing Tests

The purpose of dowel bearing tests is to determine the resistance of a specific wood species to deformation when loaded with a dowel shaped fastener. Due to the orthotropic nature of wood, the dowel bearing capacity is different when tested parallel to grain than when tested perpendicular to grain. Lower dowel bearing strength in the timbers suggest that there will be more bending-type failures of wood pegs rather than shear failures.

Twenty six dowel bearing tests were conducted on yellow poplar specimens: thirteen parallel to the grain and thirteen perpendicular grain. The tests were conducted in accordance with ASTM D5764, and followed the procedure set forth by Schmidt and MacKay (1997) and Schmidt and Daniels (1999) (Figure 2-12). Defect free 4x5x1-1/2 inch blocks were cut and then clamped together. A one-inch diameter hole was then drilled in the center. The specimens were then loaded with a one-inch steel dowel at a rate of 0.04 inches per minute using an Instron model 1332 testing machine until ultimate load was achieved. Moisture content and specific gravity tests were conducted on each specimen. During the testing of the specimens perpendicular to grain, no regard was given to the radial and tangential orientation of the grain. Load-deflection plots were developed and yield loads and stiffnesses were determined using the 5% offset method.

When loaded both parallel and perpendicular to the grain directions, dowel bearing failures were achieved in every test, unlike previous research where the parallel

to grain specimens split longitudinally. Results of the dowel bearing tests can be found in Appendix D. For parallel-to-grain loading, yellow poplar was 3.5 times stiffer and 2.2 times stronger at yield than for perpendicular to grain loading.

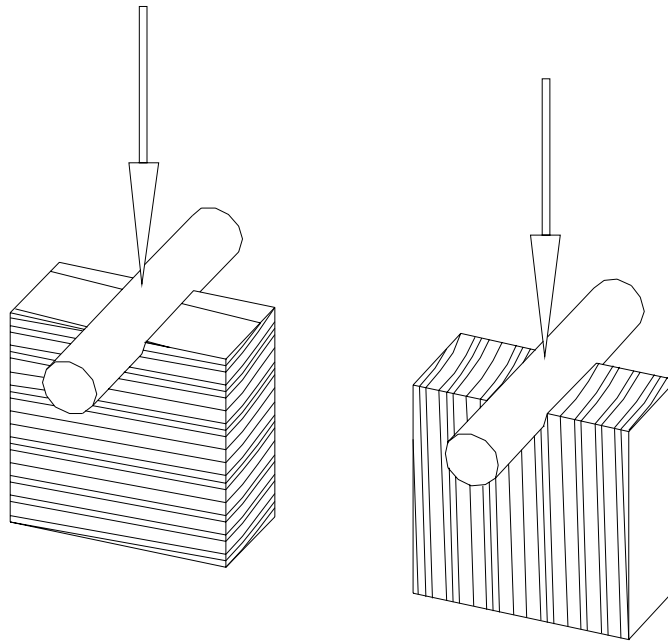


Figure 2-12 - Dowel Bearing Fixture with Loading Perpendicular and Parallel to Grain

3.0 Finite Element Modeling

3.1 Objectives

The objective of the finite element analysis was to predict the five percent offset yield load of mortise and tenon joints loaded in tension. A three-dimensional model was developed and calibrated to accurately predict the results achieved in the physical testing. Once there was sufficient confidence in the model, it was used to predict the yield loads for joints made with materials not tested physically. This aided in the development of a numerical correlation between the specific gravities and yield stress without extensive physical testing.

3.2 Model Development

The finite element modeling was conducted using ANSYS 7.1, a commercially available software program (ANSYS, 2003). The analyses were performed on a DEC Alpha 1200 5/300 dual processor computer running the UNIX operating system. A three-dimensional model was created to match the geometry of the physical tests (Figure 2-1). Detailing dimensions were 3 inches of relish (le), 3 inches of peg spacing (ls), and 3 inches of edge distance on the mortise (lv). A gap of 0.05 inches between the mortise and tenon was used to yield a net tenon thickness of 1.9 inches. This gap modeled the typical size of the gap in the yellow poplar joints at the time of physical testing. To reduce model size and computer time, symmetry boundary conditions that allowed for the modeling of one quarter of the mortise and tenon joint were employed (Figure 3-1). The

mortise and tenon were partitioned into subvolumes to facilitate meshing with 3-D brick elements.

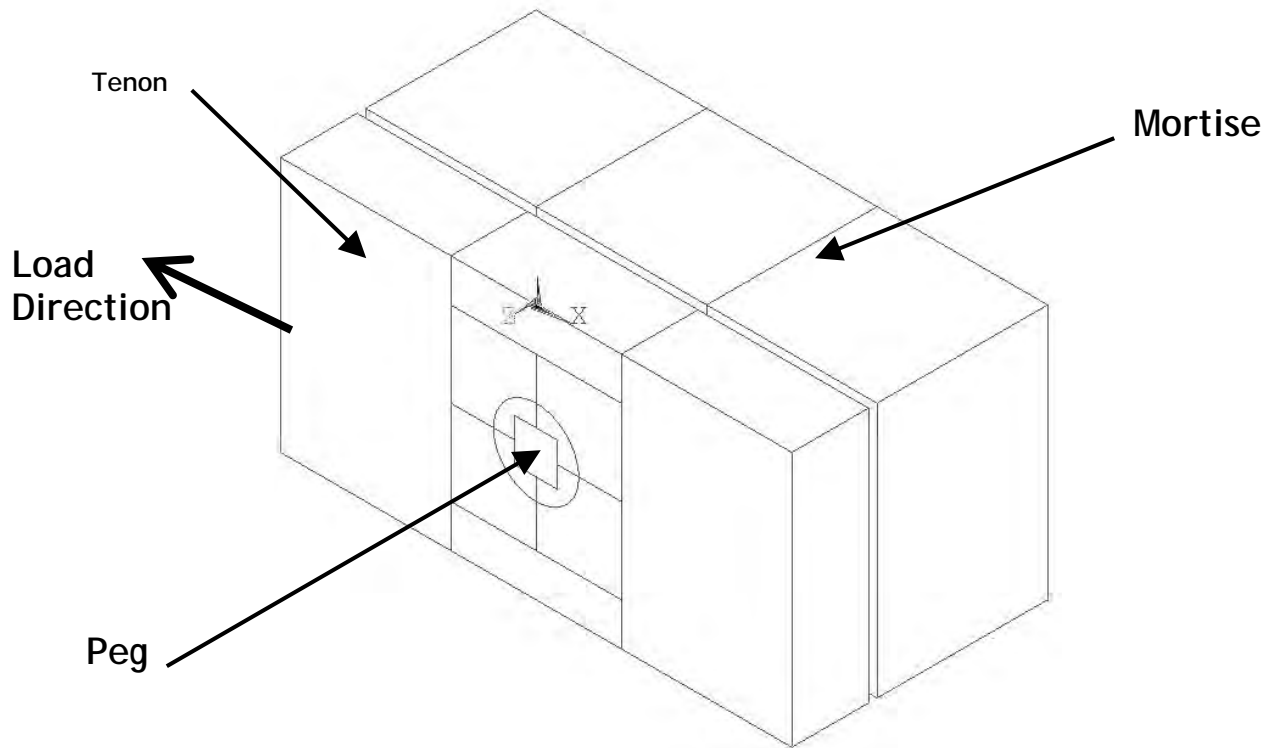


Figure 3-1- Finite Element Model Geometry for a Mortise and Tenon Joint

Orthotropic material properties for the various species of joint and peg material were taken from the Wood Handbook (Forest Products Society, 1999). The limited number of species with published shear moduli and Poisson's ratios restricted the materials that could be used in the model. Per the Wood Handbook, the published modulus of elasticity was increased ten percent to determine the elastic modulus E . This increase takes into account the shear deformations which are included with the published values. For simplicity, the same elastic modulus E was used for both the radial and

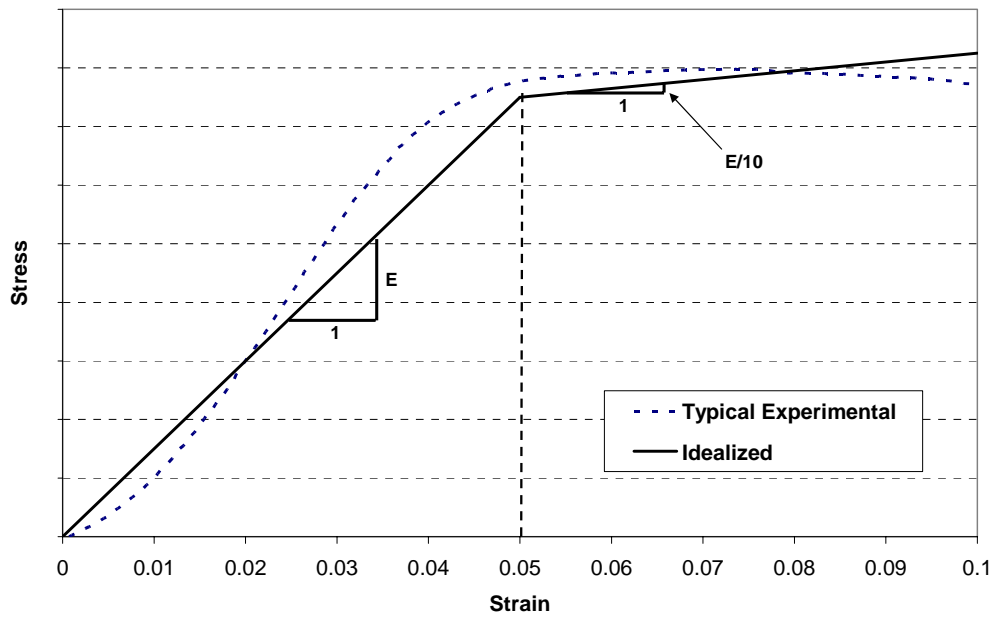
tangential directions. Likewise, a single Poisson's ratio μ was used for the radial-longitudinal and tangential-longitudinal planes.

A bilinear stress-strain relation was used to model the results from the dowel bearing tests. The initial stiffness of the material loaded parallel to grain (tenon) was the elastic modulus E with the tangent stiffness set at $0.5E$. The initial stiffness for the material loaded perpendicular to the grain (mortise and pegs) was again based on the elastic modulus, but the tangent stiffness was closer to perfectly plastic, being $0.1E$. The yield strain for the material loaded parallel to grain was 0.01 inches per inch, while the material loaded perpendicular to grain had a yield strain of 0.05 inches per inch. Figure 3-2 shows the shape of the assumed stress-strain relation compared to that from dowel bearing tests. Table 3-1 lists the material constants used. The results of the analysis were not changed significantly by variations to the tangent slope of the stress-strain curve of the base materials. However, results were very sensitive to the tangent slope of the stress-strain curve of the peg, due to the large stress concentrations in the pegs at the mortise-tenon interface. The plasticity model was based on the von Mises yield criterion, an associated flow rule, and isotropic hardening.

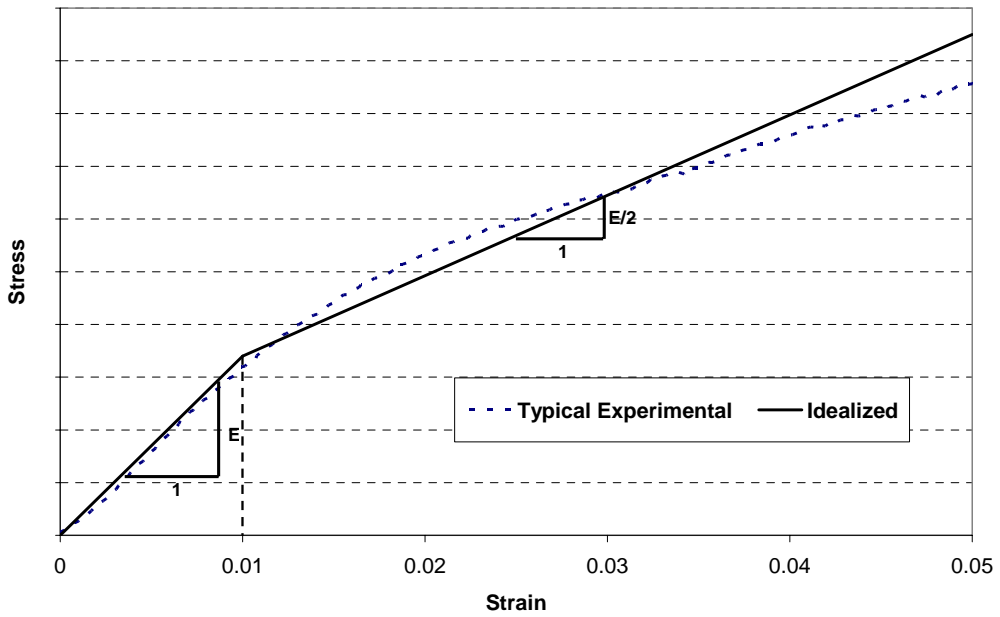
Table 3-1 - Material Properties From the Wood Handbook

Species	E_L^1 (psi)	$E_{(T \text{ or } R)}/E_L$	$G_{(LR \text{ or } LT)}/E_L$	G_{RT}/E_L	$\mu_{(LR \text{ or } LT)}$	$\mu_{(RT \text{ or } TR)}$	$\mu_{(RL \text{ or } TL)}$
E. White Pine	1,364,000	0.066	0.089	0.011	0.331	0.358	0.033
Shortleaf Pine	1,925,000	0.079	0.066	0.012	0.349	0.363	0.033
Red Oak	2,002,000	0.118	0.085	0.010	0.399	0.426	0.049
Sitka Spruce	1,727,000	0.061	0.063	0.003	0.420	0.340	0.033
White Oak	1,958,000	0.118	0.086	0.010	0.399	0.459	0.055
Yellow Poplar	1,738,000	0.068	0.072	0.011	0.355	0.516	0.025

¹ E_L is the published MOE in the Wood Handbook increased by 10%



(a) Stress-Strain Curve for Dowel Bearing Perpendicular to the Grain



(b) Stress-Strain Curve for Dowel Bearing Parallel to the Grain

Figure 3-2 - Stress - Strain Curves Used in Finite Element Modeling

A mesh refinement study was conducted to determine the coarsest mesh that could be used to obtain adequate results. Because macroscopic load-deflection behavior was the information of interest, the applied load and the deflection at a node remote from the peg location were used to evaluate convergence. A nonlinear-analysis was performed on each model under a load of 3500 pounds. Mesh refinements were conducted by changing the minimum number of divisions on the side of a volume. Some volumes had more divisions to ensure compatibility with adjacent volumes. Figure 3-3 shows the selected mesh density used for all of the models and Table 3-2 contains the results of the mesh refinement study. The decreasing joint deflection with mesh refinement can be attributed to the performance of the contact elements.

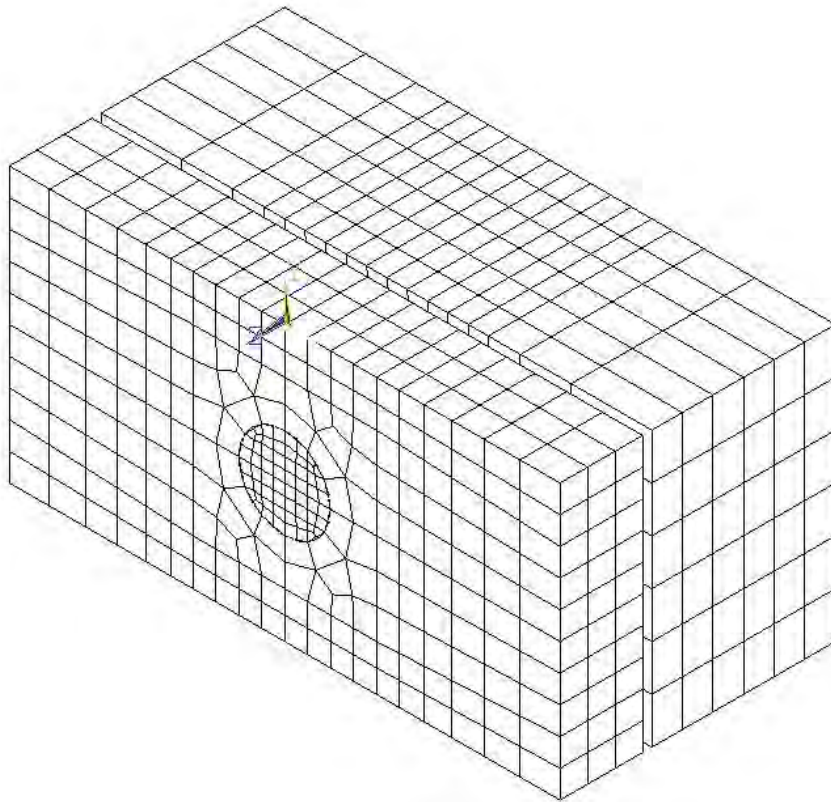


Figure 3-3 - Meshing of Mortise and Tenon Joint

Table 3-2 - Results of Mesh Refinement Study Using Orthotropic Yellow Poplar Properties and Subjected to 3500 Pounds of Load

Element Division	Number of Elements	Number of Nodes	Joint Deflection	Run Time
1	470	1,410	0.284	15 sec
2	620	2,220	0.179	2 min
3	1,082	4,830	0.139	4 min
4	2,202	10,410	0.125	12 min (Used in modeling)
5	5,040	23,820	0.123	4 hours

Twenty-node brick elements (Figure 3-4) with large-strain and non-linear capability were used with a fourteen-point integration rule to model the timber and the peg.

Contact elements were used wherever the peg might touch the mortise or tenon (Figure 3-5). The contact elements had no tensile capacity, allowing for gaps to open in various locations between the peg and the base material. Surface-to-surface contact elements were used, which allow for surface discontinuities created by different mesh densities. Figure 3-5 shows a detail of the peg / base material interface with the contact elements that create compatibility between the two meshes.

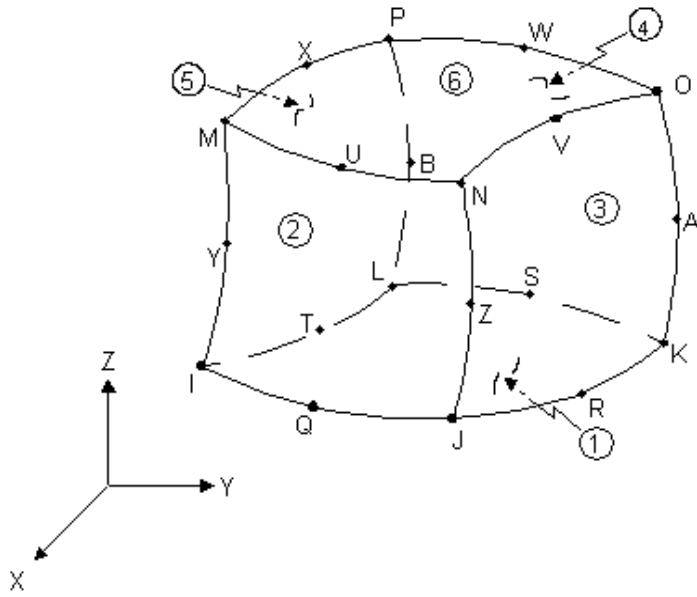


Figure 3-4 - 20-node Brick Element (ANSYS, 2003)

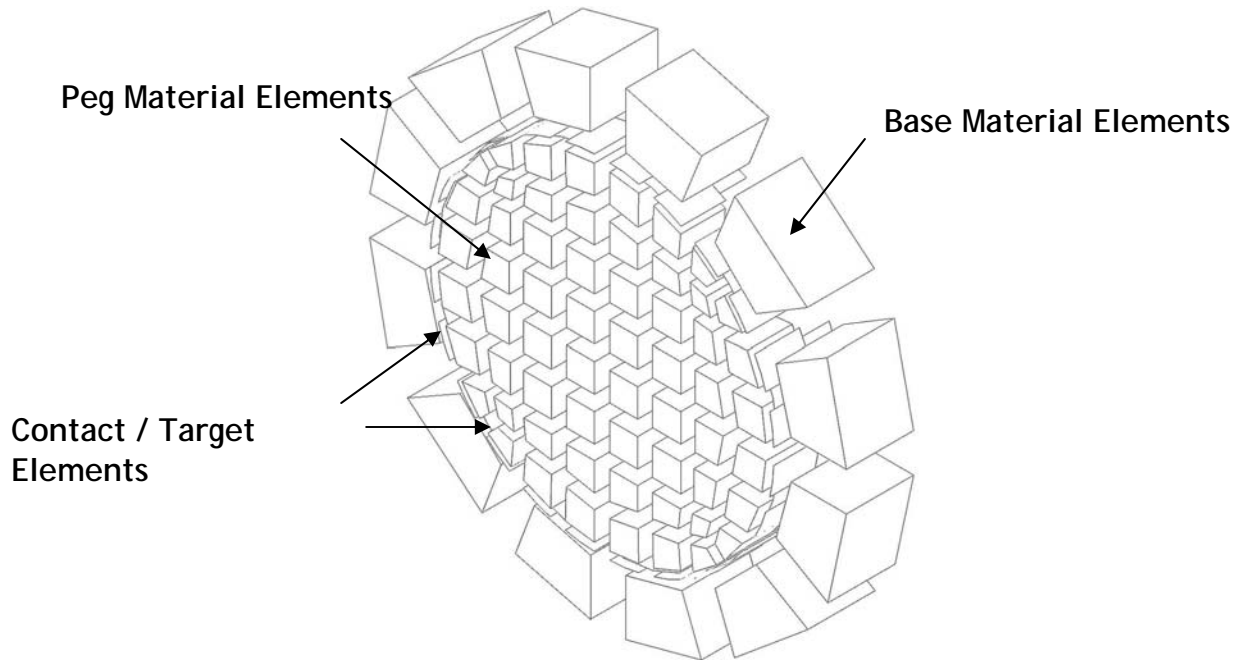


Figure 3-5 - Detail of Contact and Target Elements Near Peg

After confirming that the model performed appropriately with linear isotropic and linear orthotropic material properties, the non-linear stress-strain data was added into the base model. The same geometric model was repeatedly modified with material properties for the different species combinations. The tenon thicknesses in the physical tests with oak timber were 1.5 inches. The model geometry was modified to take this into account. The high dowel bearing capacity of the oak caused peg shearing type failures and thus the thickness of the tenon had little effect on the yield strength.

Displacement constraints along symmetry planes were employed. The nodes along the bottom of the mortise were confined from displacement. A unit pressure was applied over the cross sectional area of the tenon. The average deflection of the nodes over that area was recorded with the applied load to form a point on the load-deflection curve. The load was incremented until yield occurred. The five-percent offset method was used to determine the yield load for each joint model, at which point the analysis was terminated.

3.3 Results

The model was calibrated by slightly modifying the yield strain of the stress-strain curve. The changes were all within the variance of the stress-strain data from the dowel bearing tests. Once the model was calibrated for yellow poplar, the stress-strain function was not modified for the subsequent eight tests.

The yield load from the finite element models of the pegged mortise and tenon joints corresponded well with those from physical testing, while the joint stiffnesses from the models were softer than those from physical tests. The models tended to slightly over

predict yield loads of higher strength joints while providing a lower bound for the lower strength joints. Three joints of Douglas fir, sitka spruce, and eastern white pine were modeled with just white oak pegs. The red oak, yellow poplar, and shortleaf pine joints contained both red and white oak pegs. Table 3-3 provides a numerical comparison of some physical and modeled joints. Figure 3-7 through Figure 3-11 show load deflection plots compared to physical data for joints tested with white oak pegs.

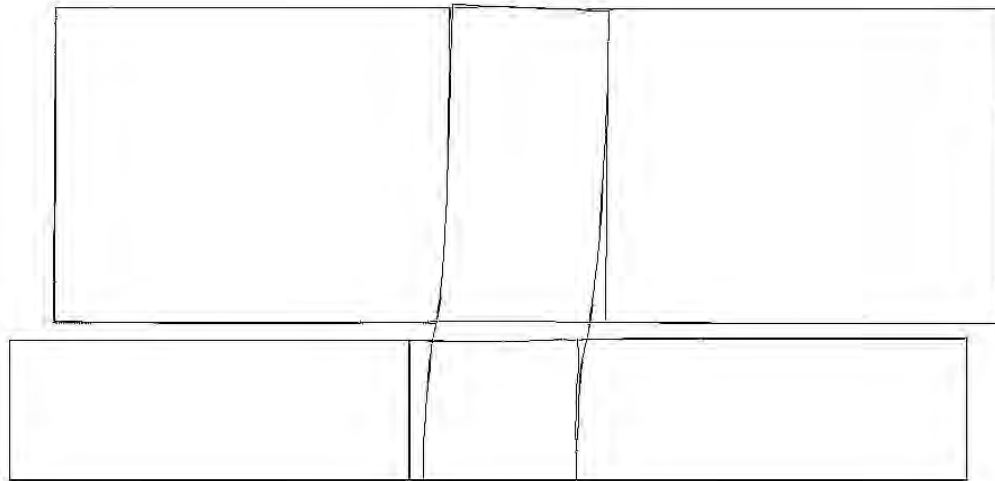


Figure 3-6 - Displaced Shape of the Joint

Table 3-3 - Comparison of Physical and Modeled Joints

Species	Physical	Modeled	Ratio	Physical	Modeled	Ratio
	Yield Load	Yield Load		Stiffness	Stiffness	
Douglas Fir	5,900	7,540	0.78	62,300	32,860	1.90
E. White Pine	4,963	4,450	1.12	55,100	23,510	3.52
Red Oak	7,374	8,428	0.87	69,710	38,140	1.83
Shortleaf Pine	7,188	7,458	0.96	82,800	32,760	2.53
Yellow Poplar	5,995	5,450	1.10	62,790	34,810	1.80

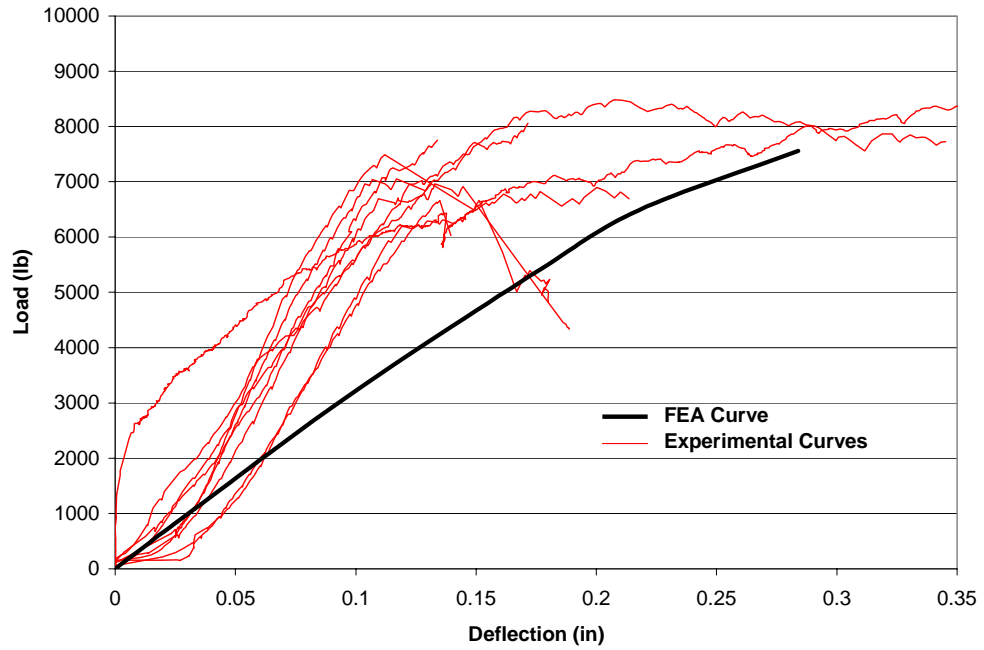


Figure 3-7 - Shortleaf Pine Physical and Modeled Load-Deflection Curves

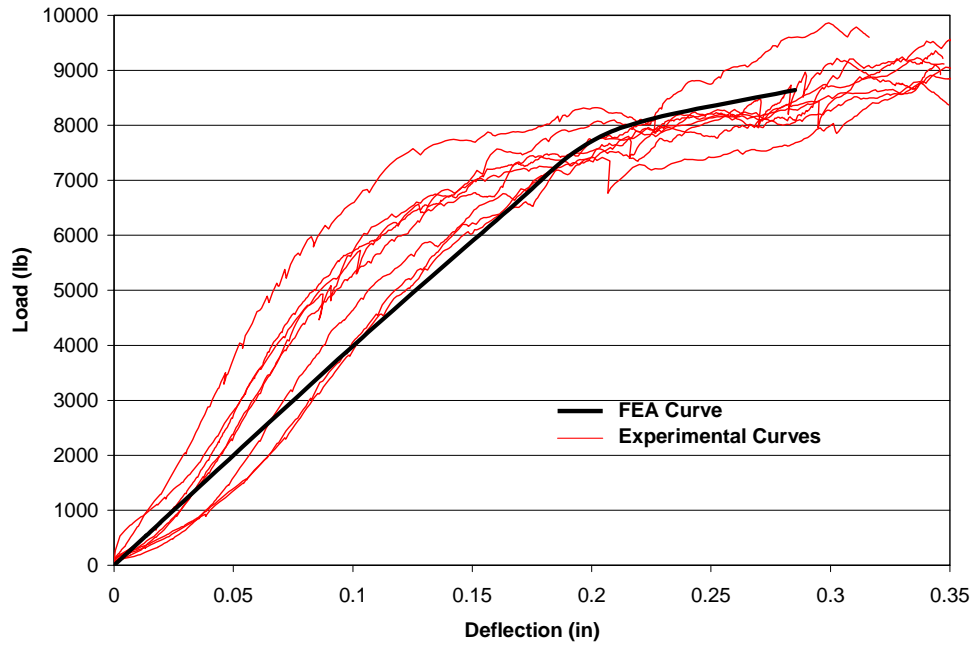


Figure 3-8 - Red Oak Physical and Modeled Load-Deflection Curves

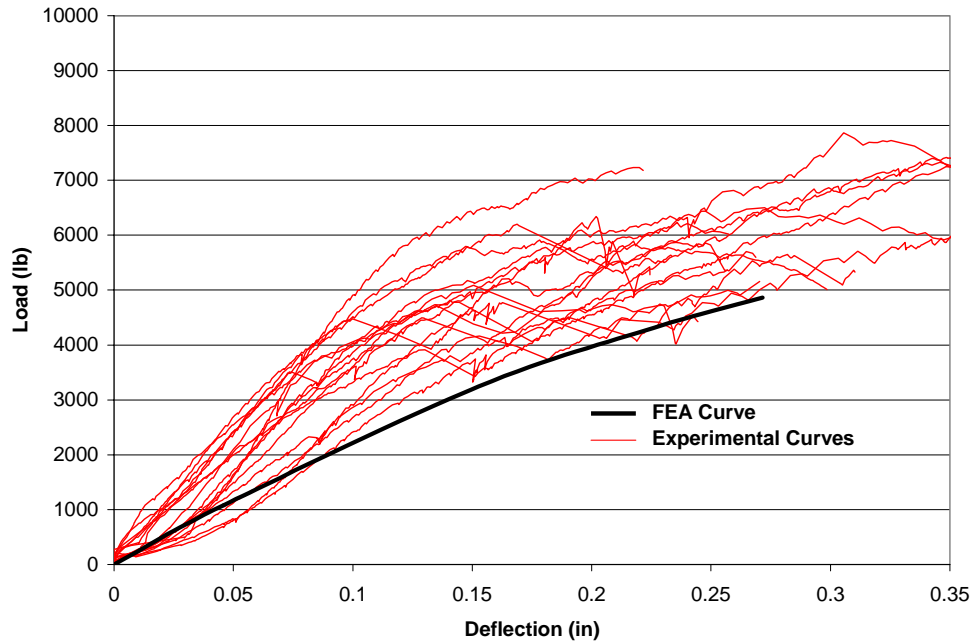


Figure 3-9 - Eastern White Pine Physical and Modeled Load-Deflection Curves

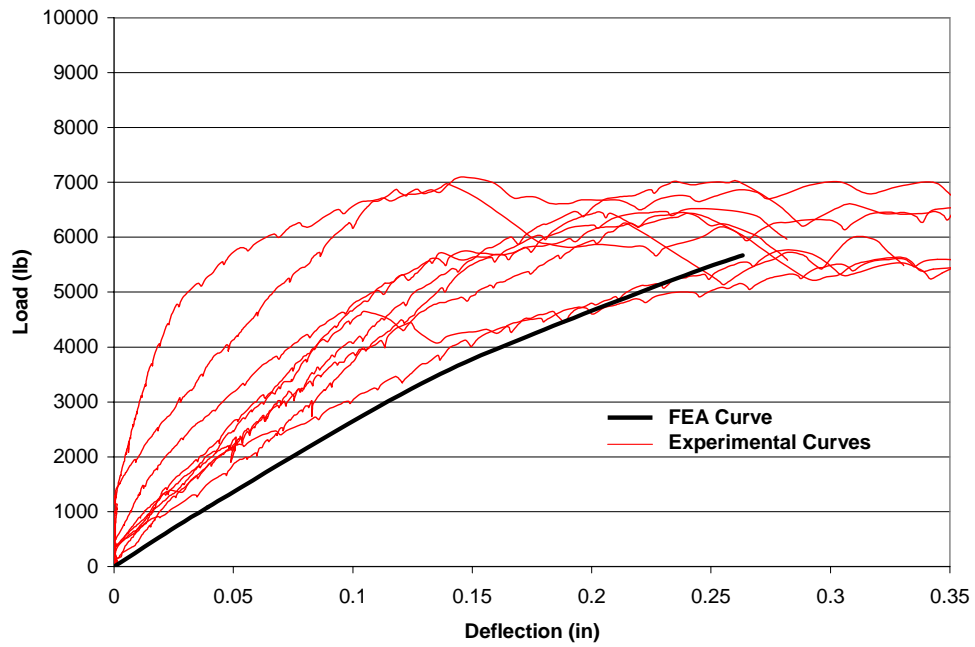


Figure 3-10 - Yellow Poplar Physical and Modeled Load-Deflection Curves

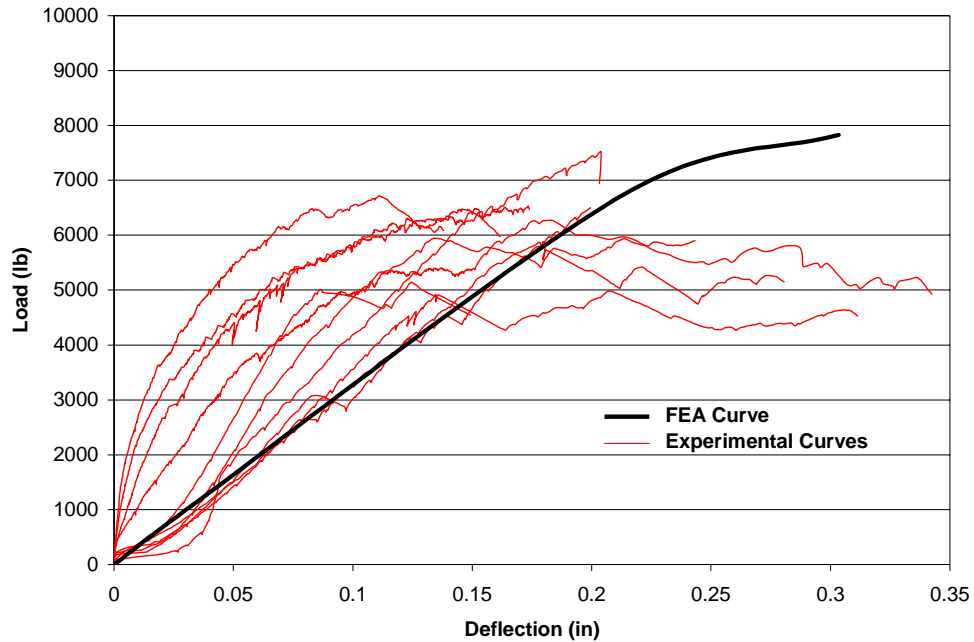


Figure 3-11 – Douglas Fir Physical and Modeled Load-Deflection Curves

3.4 Direct Bearing Joints

A finite element model was also created for a mortise and tenon joint loaded in shear. That is to say, a shear load was applied to the tenon member such that the tenon would bear directly on the bottom of the mortise. The geometry used in modeling the direct bearing joints followed what was physically tested. To accurately represent the physical tests, the shoulder of the tenon was kept 0.1 inches from the face of the mortised member. The entire length of the tenoned member was included in the model. A single plane of symmetry was used in the model, allowing for one-half of the joint to be modeled (Figure 3-12). Orthotropic material properties were used as in the tensile joint model described above, except both materials followed the bilinear stress-strain distribution with the tangent stiffness of one-half the initial stiffness. The tangent

stiffness had minimal effect on the modeling due to the low strains that were developed. In addition to the physically tested yellow poplar, models were created for eastern white pine, shortleaf pine, and white oak to provide results for a good range of specific gravities. Twenty-node brick and contact elements on the bearing surfaces of the tenon and mortise were again used. No mesh refinement study was conducted, because the same mesh density was used as in the pegged joint models, which had adequate resolution.

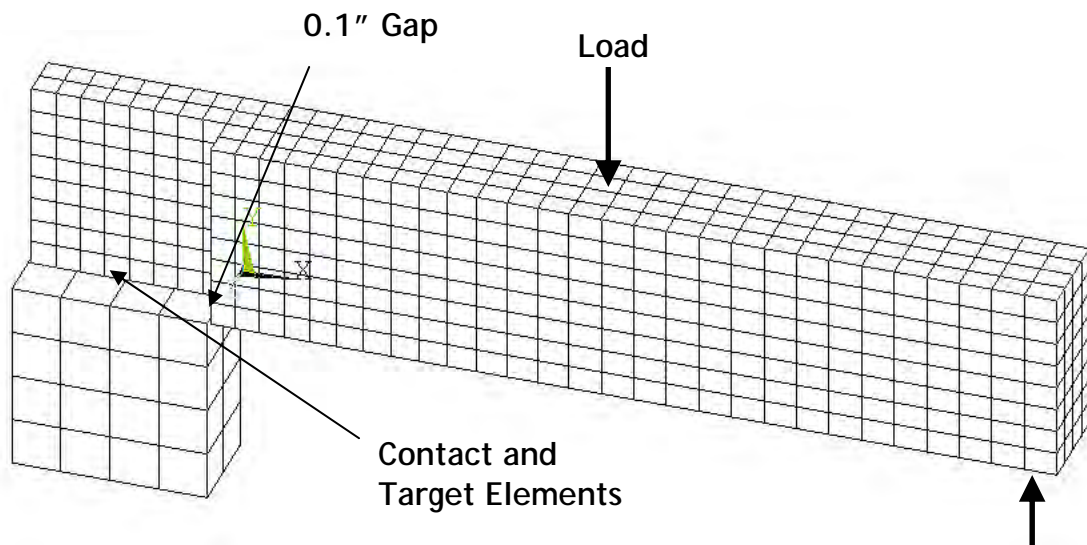


Figure 3-12 - Meshing of Direct Bearing Mortise and Tenon Joint

Load was applied to the model as a pressure in the same area that the load bearing plate contacted the tenoned member in the physical test. A node was included in the model at the same location at which the string potentiometer was connected in the physical test, and the deflections for the load-deflection curves were taken from that point. Figure 3-13 shows the modeled yellow poplar load-deflection plot along with the physical test data. Figure 3-14 shows the behavior for the other species.

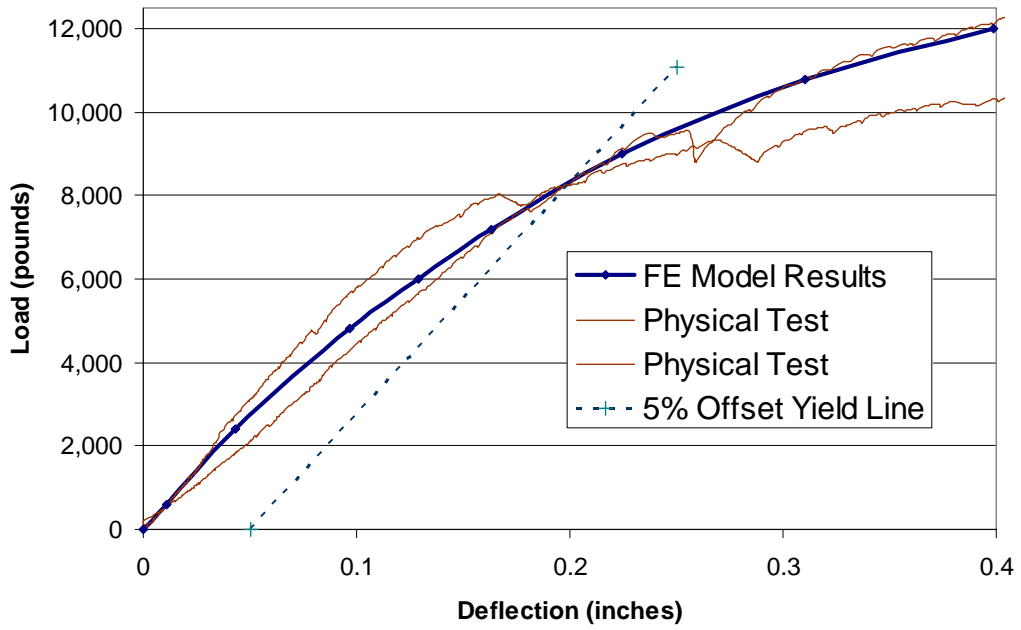


Figure 3-13 - Experimental and Modeled Direct Bearing Yellow Poplar Joints

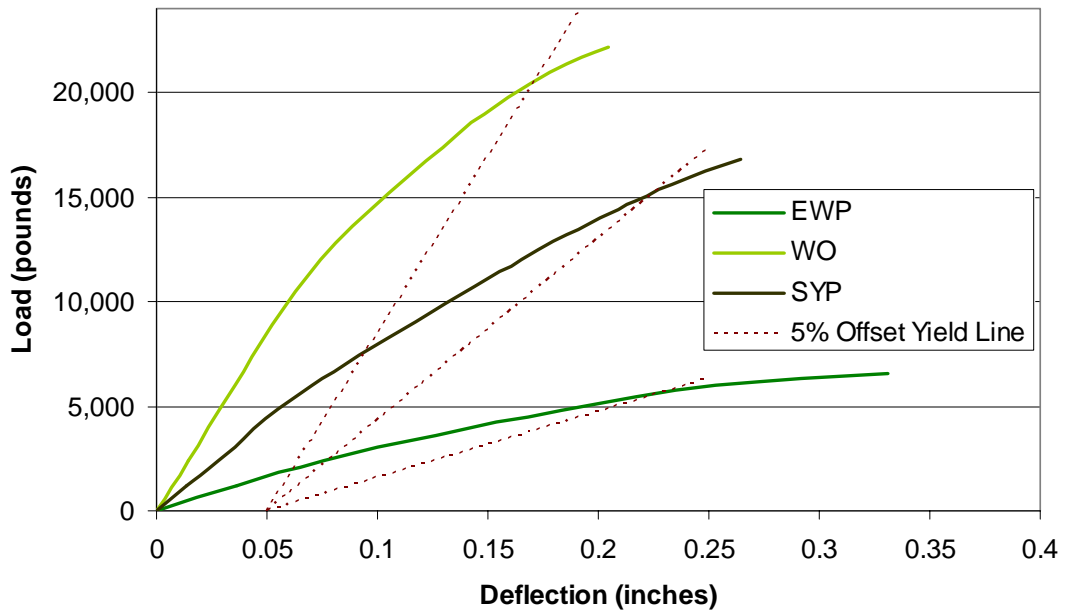


Figure 3-14 - Modeled Direct Bearing Curves for Various Species

4.0 Specific Gravity and Yield Stress Correlation

4.1 Background

With the revived interest in timber framing and the increasing desire for performance based design of these structures, a method for confidently designing mortise and tenon joints is of significant value. A correlation between the specific gravity of the materials and the joint's strength was developed to allow for easy prediction of the joint yield load. The inherent cost in time and materials associated with testing full-sized timber joints limits the number of combinations of peg and base material that can be tested. Some species, while of particular local interest, are not commonly used nationwide, and therefore are not cost efficient for testing.

Previous research at the University of Wyoming on pegged mortise and tenon joints loaded in tension included joints made of red oak, Douglas fir, shortleaf pine, and eastern white pine with various peg species. Combined with the yellow poplar testing conducted with this research, test results for a spectrum of specific gravities are available. Finite element modeling provided data to fill in the small gaps in specific gravity not covered by the physical testing. By combining these results and applying statistical curve fitting methods, an equation that describes the shear yield stress was found.

Dowel bearing strength is directly related to specific gravity (Wilkinson, 1991). A denser material has higher dowel bearing strengths, and thus produces a stronger joint. Testing was conducted on joints connected with two pegs, each in double shear. This resulted in four shear planes being loaded. By considering only the cross-sectional area

of the pegs in the shear planes (Figure 4-1), a numerical correlation based on shear stress and the specific gravities of the peg and base materials is possible.

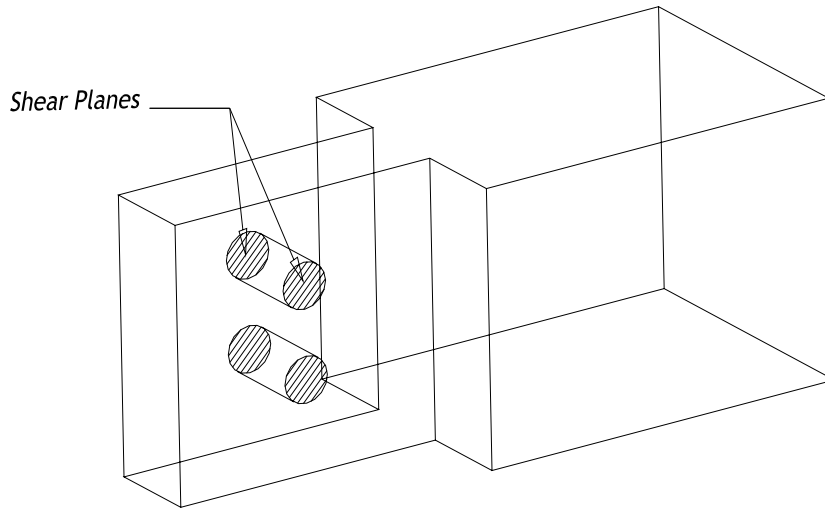


Figure 4-1 - Four Shear Planes Used in Converting Yield Load to Yield Stress

4.2 Development

Regression of the specific gravity data into an equation that predicted the shear yield stress began by selecting an equation type that fit the shape of the data. With three variables involved (the specific gravity of the pegs, the specific gravity of the base material, and the joint yield stress), the equation describes a surface rather than a line. A multi-variable power equation

$$F_{vy} = \alpha G_{PEG}^{\beta} G_{BASE}^{\gamma} \quad \text{Equation 4-1}$$

was chosen to follow the form of the equations relating specific gravity to dowel bearing strength published in the NDS. Other types of correlation functions were also investigated, yet the power curve was the most accurate and simplest in form. In

Equation 4.1, where F_{vy} is the shear yield stress (psi), G_{PEG} is the specific gravity of the peg, G_{BASE} is the specific gravity of the base material, and α, β, γ are constants.

A least squares regression was used with the data to minimize the error of the surface and determine the constants. A coefficient of determination, also known as the R^2 value, was the guideline for the goodness of fit. Appendix E includes the MathCAD worksheet with the calculations.

4.3 Results

Table 4-1 shows the specific gravities and yield stresses used for determining the correlation, along with the predicted value from the correlation. The experimental data included specific gravity data taken during physical testing. For the finite element data, specific gravity values were taken from the NDS (AFPA, 2001). The NDS's specific gravity values are slightly higher than those published for the same species in the Wood Handbook. Therefore, using the NDS specific gravities is a conservative approach when developing the correlation.

The regression analysis of the data in Table 4-1 gave the relation

$$F_{vy} = 4810 G_{PEG}^{0.926} G_{BASE}^{0.778} \quad \text{Equation 4-2}$$

in which F_{vy} is the shear yield stress in psi. This correlation had a coefficient of determination of 0.803. Figure 4-2 shows the data in Table 4-1 plotted along with the resultant correlation surface. Figure 4-3 shows the correlation surface and data plotted on edge to illustrate the deviation of each point from the surface.

Table 4-1 - Specific Gravity and Yield Stress Data Used in Developing the Correlation

Test Method	Material		Specific Gravity		Yield Load (lb)	Yield Stress (psi)	Yield Stress (Equation) (psi)	Difference %
	Peg	Base	Peg	Base				
Physical	W. Oak	S. Pine	0.74	0.45	7,190	2,290	1,980	13.6%
Physical	R. Oak	S. Pine	0.64	0.48	5,360	1,600	1,810	-13.0%
Physical	W. Oak	Doug. Fir	0.64	0.48	5,900	1,880	1,770	5.5%
Physical	W. Oak	Red Oak	0.77	0.66	7,370	2,440	2,720	-11.2%
Physical	W. Oak	E. White Pine	0.75	0.35	4,960	1,610	1,620	-0.7%
Physical	W. Oak	Y. Poplar	0.66	0.45	5,600	1,910	1,760	7.8%
F.E. Model	W. Oak	Y. Poplar	0.73	0.43	5,450	1,740	1,860	-7.4%
F.E. Model	W. Oak	Red Oak.	0.73	0.68	8,430	2,680	2,660	0.8%
F.E. Model	W. Oak	E. White Pine	0.73	0.36	4,450	1,420	1,620	-14.6%
F.E. Model	W. Oak	White Oak	0.73	0.73	8,450	2,690	2,810	-4.6%
F.E. Model	W. Oak	Shortleaf Pine	0.73	0.59	7,460	2,370	2,380	-0.4%
F.E. Model	W. Oak	Doug. Fir	0.73	0.50	7,540	2,400	2,100	12.7%
F.E. Model	R. Oak	R. Oak	0.68	0.68	7,790	2,480	2,490	-0.5%
F.E. Model	R. Oak	Y. Poplar	0.68	0.43	5,240	1,670	1,750	-4.7%
F.E. Model	R. Oak	Shortleaf Pine	0.68	0.51	6,340	2,020	1,990	1.2%

The correlation was based on white oak and red oak peg data, with the peg always of equal or higher density than the base material. The ranges of specific gravities for the pegs and timbers were from 0.64 to 0.77 and 0.36 to 0.73, respectively. Therefore, a usable specific gravity range of 0.6 to 0.8 for the pegs and from 0.35 to 0.75 for the timbers is reasonable. Testing outside the current specific gravity ranges is recommended before the ranges of specific gravity are expanded.

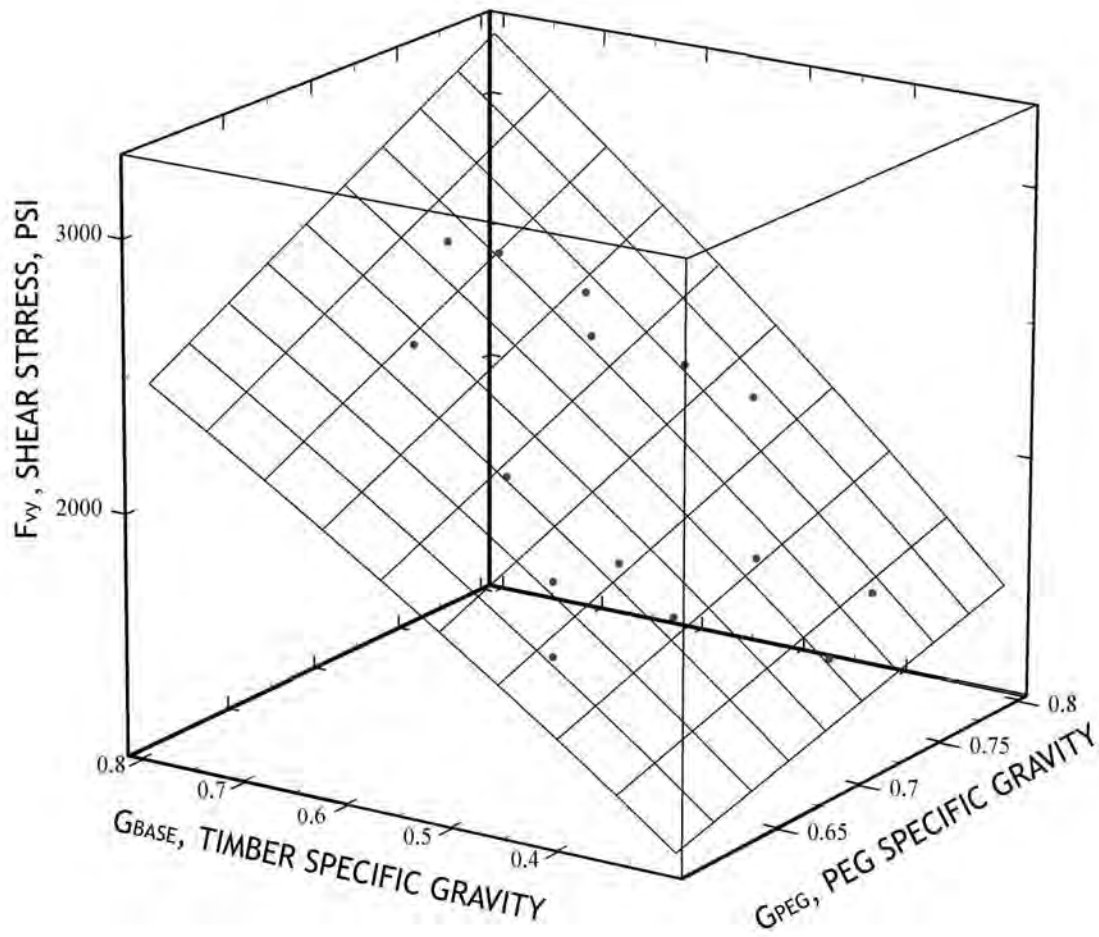


Figure 4-2 - Plot of Yield Points with Correlation Surface



Figure 4-3 - Correlation Surface and Data Points Viewed Along Edge

5.0 Design of Mortise and Tenon Joints

5.1 Introduction

The correlation between specific gravity of the joint materials and the shear yield stress of a mortise and tenon joint provides the necessary foundation for developing a design procedure. The most direct and logical approach is to apply a factor of safety to the yield stress correlation. The selection of an appropriate factor of safety for these traditional joints will yield a safe yet simple design equation.

Since 1991, the NDS (AFPA, 2001) has used the European Yield Model to predict the strength of dowel-type connections with steel fasteners. The EYM is an ultimate strength model and predicts the load capacity of a joint, assuming elastic perfectly-plastic behavior. The bending strength of the dowel as well as the dowel bearing strength of the timber are used in the EYM. These material properties are based on the five-percent offset yield method.

5.2 Selection of a Factor of Safety

Kessel and Augustin (1996) conducted work in Germany to develop tensile capacities and appropriate factors of safety for pegged mortise and tenon joints. Their factors of safety were selected for a particular size joint with a particular timber and peg species. They recommended that the design load for the joint be the lesser of:

- The mean value of the ultimate loads divided by a factor of safety of 3.0.
- The mean value of the loads at 1.5 mm of deflection, approximately one-half the proportional limit, with a factor of safety of 1.0.

- The absolute minimum ultimate load divided by a factor of safety of 2.25.

One method for developing a factor of safety would be to modify Kessel and Augustin’s recommendations. However, their recommendation of 3.0 for the factor of safety was based on the mean ultimate load, not the yield load. The average ratio of the five-percent offset yield load to the ultimate load of the joint for all of the physical testing conducted at the University of Wyoming is 0.83, as can be see in Table 5-1. Decreasing Kessel’s mean ultimate load factor of safety of 3.0 by this ratio yields a factor of safety of approximately 2.5.

Table 5-1- Ratio of Yield Load to Ultimate Load for Full-Sized Joints

Southern Yellow Pine	0.755
Yellow Poplar	0.870
Douglas Fir	0.870
Red Oak	0.809
Eastern White Pine	0.850
<hr/> Average	<hr/> 0.831

The basis of Kessel’s factor of safety of 3.0 is not discussed in his report (Kessel & Augustin, 1996). It may be based on historical precedence or other research. Without knowing the basis for the factor of safety, one cannot easily suggest design recommendations based upon it.

Schmidt and Daniels’ (1999) research included an investigation into which factor of safety was appropriate for mortise and tenon joints. His suggestion was a factor of safety of 2.0. This suggestion was based on a relationship he developed between the shear span and shear stress of the peg at yield. The specific gravity correlation developed

with current research is not based on the shear span of the peg, and therefore a factor of safety of 2.0 may not be appropriate.

A logical approach for developing a new factor of safety would be to use the current EYM equations in the NDS as a baseline. Research conducted by Reid (1997) suggested that Mode IIIs failure of the EYM accurately represented physical tests of mortise and tenon joints with wood pegs. In addition, the failure mode of most pegged mortise and tenon joints at the University of Wyoming was also Mode IIIs. The ratio of the yield load predicted by the correlation in Equation 4-2 to the Mode IIIs allowable joint load should provide a factor of safety that has the same performance as the current design procedures (Table 5-2).

Table 5-2 - Ratio of Correlation Strength to EYM Mode IIIs Allowable Load

Test Method	Material		Specific Gravity		Correlation Yield Load (lb)	Mode IIIs Allowable (lb)	Yield Allowable
	Peg	Base	Peg	Base			
Physical	W. Oak	S. Pine	0.74	0.45	3,072	1,297	2.37
Physical	R. Oak	S. Pine	0.64	0.48	2,824	1,369	2.06
Physical	W. Oak	Doug. Fir	0.64	0.48	2,824	1,369	2.06
Physical	W. Oak	Red Oak	0.77	0.66	4,293	1,926	2.23
Physical	W. Oak	E. White Pine	0.75	0.35	2,558	1,063	2.41
Physical	W. Oak	Y. Poplar	0.66	0.45	2,763	1,297	2.13
F.E. Model	W. Oak	Y. Poplar	0.73	0.43	2,928	1,249	2.34
F.E. Model	W. Oak	Red Oak.	0.73	0.68	4,182	1,986	2.11
F.E. Model	W. Oak	E. White Pine	0.73	0.36	2,550	1,086	2.35
F.E. Model	W. Oak	White Oak	0.73	0.73	4,419	2,138	2.07
F.E. Model	W. Oak	Longleaf Pine	0.73	0.59	3,745	1,644	2.28
F.E. Model	W. Oak	Doug. Fir	0.73	0.5	3,292	1,418	2.32
F.E. Model	R. Oak	R. Oak	0.68	0.68	3,916	1,986	1.97
F.E. Model	R. Oak	Y. Poplar	0.68	0.43	2,742	1,249	2.19
F.E. Model	R. Oak	Longleaf Pine	0.68	0.59	3,507	1,644	2.13

Average (Factor of Safety) 2.20

The ratio of the Equation 4-2 correlation yield load to the EYM Mode IIIs allowable load is 2.20. This is the factor of safety associated with the correlation yield

load when compared to the current NDS standard. Hence, a factor of safety of 2.2 is recommended for use with Equation 4-2 to determine an allowable design value for peg shear in mortise and tenon joints.

5.3 Load Duration Factor

Long standing research (Wood, 1951) has demonstrated that the strength of wood flexural members is sensitive to the duration of the load; strength decreases as load duration increases. Hence, the NDS permits adjustment of many wood design values, including those for connection design, by load duration factors. These load duration factors are based on the Madison curve (Figure 5-1), which calibrates all loads relative to a duration of ten years (AFPA, 2001).

Physical testing in this research was based on a load-to-failure time of approximately ten minutes. The load duration factor for ten-minute loading is 1.6. The design equation being developed therefore should be reduced by a factor of 1.6 for adjustment to the standard ten-year load duration.

Schmidt and Scholl's research on the long-term behavior of loaded mortise and tenon joints with wood pegs included suggestions for a load-duration factor of 1.0 for joints loaded under long term. The recommendation was based on testing of joints that had been subjected to a static long-term service-level loading.

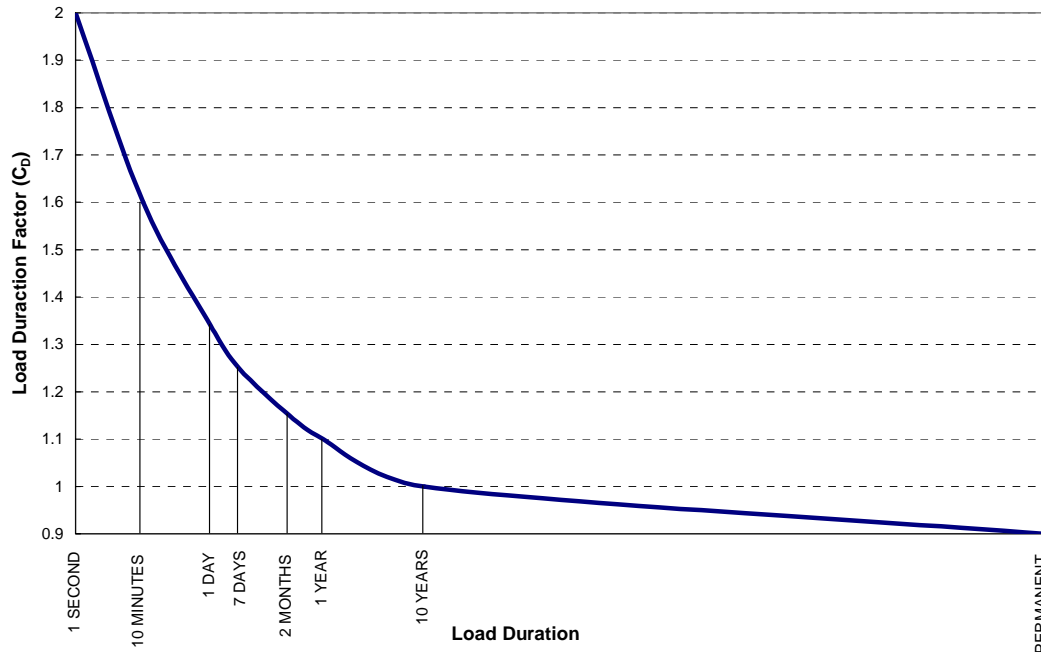


Figure 5-1 - Madison Curve Showing Load Duration Factors

Recent work conducted by Bulleit and his colleagues found that load duration factors for connections may not be the same as the load duration factors for flexure (Bulleit et al, 2000). From their research, heavily loaded joints failed at loads below the predicted values, suggesting the load duration factors for connections are slightly unconservative. Their research indicated that load duration factors for heavily loaded joints should be decreased by 9 percent, while those for moderately loaded joints should be decreased 4 percent. However, Bulleit's testing was conducted on small samples, which are more susceptible to moisture variations that increase the creep rate in wood. This suggests that the observed load duration factors may be lower than what is

experienced in larger joints. Therefore, until further testing is conducted, Bulleit recommends that the standard load duration factors be used with connections.

5.4 Design Equation

Incorporating the factor of safety of 2.20 and removing the load duration factor of 1.6 from the first constant of the yield stress correlation equation (Equation 4-2) gives the design equation

$$F_v = 1365 G_{PEG}^{0.926} G_{BASE}^{0.778} \quad \text{Equation 5-1}$$

where F_v is the allowable shear stress in the peg in psi. G_{PEG} is limited to the range of 0.6 to 0.8 and must always be higher than G_{BASE} . G_{BASE} is limited to the range of 0.35 to 0.75. The load duration factor was included so the design equation reflects a standard load duration of ten years. The designer can conservatively use the equation as is, or can increase the allowable stress by the load duration factor, as permitted by the NDS. This equation can be safely and confidently used for the design of pegged mortise and tenon joints loaded in tension. A design example is included in Table 5-3.

Table 5-3 - Example on the Proper Usage of the Correlation

Example Design Usage of Correlation		
G_{PEG}	0.73	(White Oak)
G_{BASE}	0.43	(Yellow Poplar)
Number of Pegs	2	
Peg Diameter	1	inches
Load Duration	1.6	(Wind Load - Per the NDS)
Shear Stress	529	lb/in ² (per EQ. 5-1)
Shear Area	3.142	in ²
Joint Capacity	2659	lb

6.0 Utilization of Yellow Poplar

6.1 General Information

Yellow poplar is an eastern hardwood with a growth area that ranges from Florida to New York and westward to Illinois (Figure 6-1). It is a fast-growing tree that can reach up to 160 feet in height. It has few branches until well up the straight bole, and is usually less susceptible to disease. The wood ranges from whitish sapwood (sometimes called white wood) to yellow/tan heartwood that is occasionally streaked with non-strength-affecting purple and green stains. The leaves are shaped in a tulip fashion, which give the species the common nickname of tulip poplar. Currently, yellow poplar is most commonly used for interior painted trim work and pulpwood. However, most turn-of-the-century covered bridges in Indiana and Ohio were constructed of yellow poplar, as were many in other eastern states. This history of use in heavy-timber construction strongly suggests its suitability as a timber framing material.



Figure 6-1 - Natural Range of Yellow Poplar (FS-272)

6.2 Availability

Production of yellow poplar lumber reached an all time high in 1899 with 1,118 million board feet produced, and production has since declined to 847 million board feet (FS-272). Growth of yellow poplar lumber has increased to 2,137 million board feet per year, meaning a net growth of 1,290 million board feet per year. This makes yellow poplar one of the most abundant hardwoods, and it is becoming more and more abundant each year. Due to yellow poplar's abundance, its price is relatively low. Green squared timbers are currently available for a cost of \$45 to \$50 per thousand board feet; about half the cost of oak.

6.3 Material Properties

6.3.1 Strength

The NDS does not include design values for timber sized pieces of yellow poplar despite being of commercial importance. However, dimension lumber values are provided, and these values will be used for comparison's sake. Yellow poplar is in the lower third of hardwoods when it comes to specific gravity, bending strength, toughness, shear strength and tensile strength. The modulus of elasticity of yellow poplar is 36 percent higher than that of white oak, and it weighs only 58 percent as much. In many cases in design, serviceability controls member size selection. Therefore, a stiffer material such as yellow poplar with lower self weight than oak can be of great interest.

The faster yellow poplar grows, the stronger it is (FS-272, 1985). Old growth yellow poplar, which grew more slowly, tends to be lighter and weaker than second-growth material. Yellow poplar from wet, temperate climates grows the fastest and is the

strongest. As the density of yellow poplar increases, so does its strength, and in turn the color of the heartwood becomes a darker yellow.

Joint testing at the University of Wyoming suggests that yellow poplar is a viable wood for use as a timber framing material based on strength parameters. The average yield load for yellow poplar joints with a peg specific gravity of 0.66 was 5995 pounds. The average yield load for Douglas fir joints with a peg specific gravity of 0.64 was 5900 pounds. This suggests that fast-growing, dense yellow poplar is comparable in strength to Douglas fir when used in a mortise and tenon joint.

6.3.2 Drying

Yellow poplar typically exceeds 100 percent moisture content when cut and it shrinks quickly. Even though yellow poplar decreases its void ratio the faster it grows, it also increases its vessel area. This vessel area is directly related to the longitudinal permeability (Chen et al, 1998). Higher permeability increases the drying rate, thus making yellow poplar one of the quickest drying hardwoods. This characteristic makes yellow poplar suitable for kiln-drying, since little time is needed to reach equilibrium moisture content. Once dried, yellow poplar is a dimensionally stable wood, in certain cases twice as stable as red oak (Table 6-1).

Table 6-1 - Dimensional Change in 3" Lumber (in inches) (Forest Products Lab, 2000)

MC Change	<u>Red Oak</u>		<u>Yellow Poplar</u>		<u>Ratio Y.P. to R.O.</u>	
	Radial	Tangential	Radial	Tangential	Radial	Tangential
1%	0.005	0.011	0.005	0.009	1	0.82
2%	0.014	0.033	0.014	0.017	1	0.52
3%	0.024	0.055	0.024	0.026	1	0.47

The yellow poplar used in physical joint testing at the University of Wyoming was harvested, squared, and delivered within one week. The extremely low winter equilibrium moisture content in Laramie, Wyoming (6-8%) along with the lack of any end sealer caused each of the boxed heart timbers to check to the center within 4 months. This suggests care must be taken slow the drying rate in arid climates to minimalize material degradation.

6.3.3 Workability

Yellow poplar is a very easy wood to work. Its widespread usage in interior trim and turnings attest to this. It cuts easier than most hardwoods and produces a sweet-smelling sawdust. The relatively straight- and uniform-grain make chiseling and paring easy to perform. Extensive cutting and chiseling do not noticeably dull edge tools. Yellow poplar does not sand as well as other hardwoods since it is softer, but planes to a shiny surface with relative ease.

6.4 *Conclusion on Usage*

Based on its performance in this research, its physical characteristics, and cost, yellow poplar has possibilities as a timber framing material. Wide spread usage in covered bridges bear witness to this. Its low cost, increasing availability and quick drying should make up for its lack in strength compared to other hardwoods. Therefore, yellow poplar should be considered a viable option as a timber framing material.

7.0 Summary and Conclusions

7.1 *Joint Research*

7.1.1 Physical Testing

Pegged yellow poplar mortise and tenon joints physically tested in tension behaved in a similar fashion to other tests conducted at the University of Wyoming. The same failure modes in the tenon relish and mortise cheek were observed, as were peg shearing and bending failures. Use of the same testing frame and setup procedure ensured that these tests could be directly compared with previous ones. Modification of the peg hole location during subsequent tests allowed minimum detailing requirements to be developed for yellow poplar. These detailing requirements can be added to those for other species.

Shear testing of the mortise and tenon joints, in which the tenoned member was loaded in shear and the load was transferred through the pegs, gave the expected poor capacities. Low strength in tension perpendicular to the grain results in undesirable tenon splitting failures. Large through tenons and single-peg connections were required to induce peg bending failures. When these peg failures did occur, they occurred at approximately the same yield stress in the peg as the tension testing.

Direct bearing tests of the mortise and tenon joints were performed with the tenoned member loaded in shear and the load transferred through direct bearing of the tenon on the bottom of the mortise. In these tests, the joints were much stiffer and stronger than the same joint loaded in shear through the pegs. Therefore, direct bearing, not pegs, should be used to transmit shear loads from the tenon to the mortise.

7.1.2 Finite Element Modeling

Time and materials did not permit testing a wide variety of wood and peg species, so a finite element model was developed. Once the three-dimensional model was validated against physical test results, other species of materials were modeled to round out the spectrum of specific gravities for development of a correlation between specific gravity and the yield stress of a pegged mortise and tenon joint loaded in tension.

Published orthotropic material properties and a bilinear stress-strain curve were incorporated into a three-dimensional finite element model of a mortise and tenon joint. The model provided accurate results when the desired data is the five-percent offset yield load.

7.2 *Design Equations and Correlation*

A simple correlation relating the specific gravities of the timbers and pegs to allowable yield stress was developed. The correlation was based on the direct relationship between a material's dowel bearing strength and specific gravity. From the correlation, a design equation was developed for the allowable shear stress in the pegs of a mortise and tenon joint loaded in tension. A reasonable factor of safety and load duration effects were included in the equation so that it can be used like any other allowable stress from the NDS.

The simple form of the correlation equation should allow for easy adoption by design professionals. It can be safely and accurately used within the range of specific gravities tested.

7.3 Usage of Yellow Poplar

In this research, yellow poplar proved to be a viable choice as a timber framing material. It is low cost and readily available in the eastern United States. It dries quickly with a minimal amount of degradation. The stiffness to weight ratio is higher than that of oak, and its strength in tensile loaded mortise and tenon joints is comparable to that of Douglas fir. Yellow poplar acts as a hardwood, so tenons should be detailed with a thickness of 1.5 inches.

7.4 Recommendations for Future Research

Mortise and tenon joints with peg materials other than red and white oak should be studied to allow for confidence in the developed design equation outside of the current range of specific gravities. Peg diameters other than 1.0 inch should also be tested to ensure the design yield stress is adequate for a range of peg sizes. These studies could be performed either experimentally or by the finite element method.

Loading joints at a rate to induce failure in days or weeks may be difficult to execute, but would provide good insight into the applicability of load duration factors to the yield stress equation.

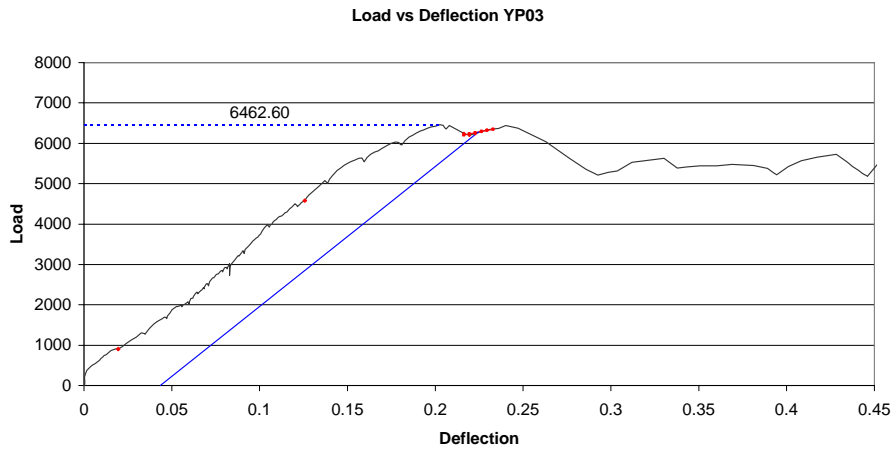
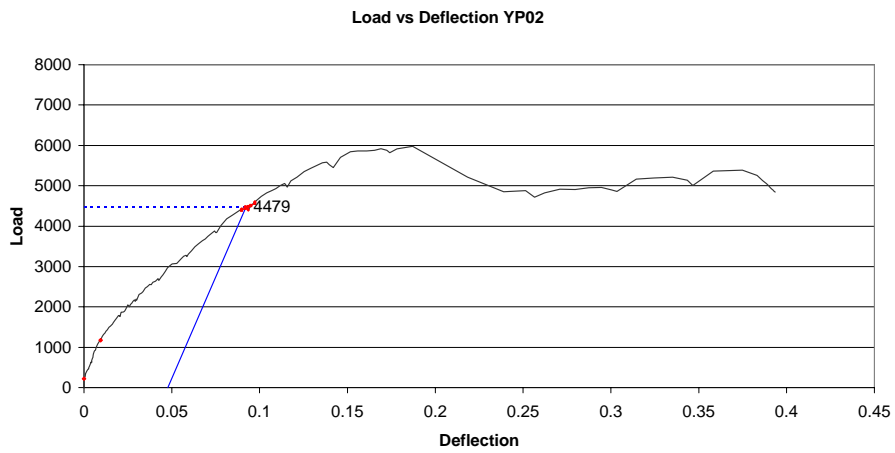
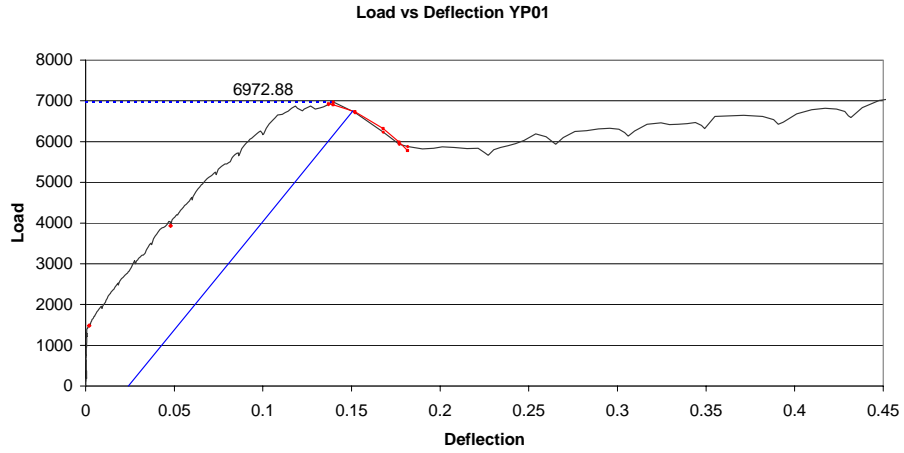
8.0 References

- AFPA, (2001). "National Design Specification for Wood Construction," American Forest and Paper Association (AFPA), Washington, DC.
- ANSYS, (2003). "ANSYS 7.1 User's Manual," SAS IP, Inc.
- Benson, T., Gruber, J., (1980). "Building the Timber Frame House." Charles Schribner's Sons, New York.
- Brungraber, R. L. (1985). "Traditional Timber Joinery: A Modern Analysis," Ph.D. Dissertation, Stanford University, Palo Alto, California.
- Bulleit, W.M., Martin, Z.A., Marlor, R.A., (2000). "Load Duration Behavior of Steel-Doweled Wood Connections," *Proceedings, World Conference on Timber Engineering, British Columbia*, 2-4-3.
- Chapra, S.C., Canale, R. P., (1998). "Numerical Methods for Engineers, 3rd Edition," McGraw Hill, Boston.
- Chen, C.J., Lee, T.L., Jeng, D.S., (2003). "Finite Element Modeling for the Mechanical Behavior of Dowel-Type Timber Joints," *Computers and Structures*, 81, 2731-2738.
- Chen, P., Zhang, G., Van Sambeek, J.W., (1998). "Relationships Among Growth Rate, Vessel Lumen Area, and Wood Permeability for Three Central Hardwood Species," *Forest Products Journal*, 48:3, 87-90.
- Drewek, M.W. (1997). "Modeling the Behavior of Traditional Timber Frames," M.S. Thesis, Michigan Technological University, Houghton, Michigan.
- Erikson, R.G. (2003). "Behavior of Traditional Timber Frame Structures Subjected to Lateral Load," Ph.D. Dissertation. University of Wyoming, Laramie, Wyoming.
- Forest Products Laboratory, (2000). "Drying Hardwood Lumber," FPL-GTR-118, Madison, Wisconsin.
- Forest Products Society, (1999). "Wood Handbook," *FPL-GTR-113*, Madison, Wisconsin.
- FS-272, (1985). "Yellow Poplar," Forest Service, United States Department of Agriculture, Washington, DC.

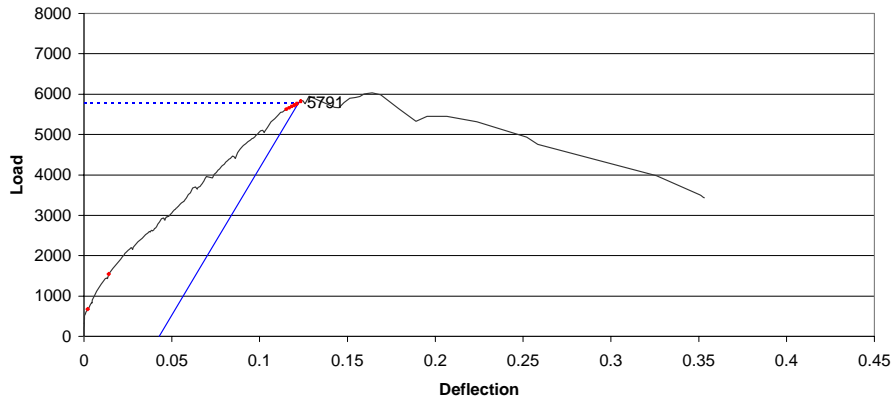
- Kharouf, N., McClure, G., Smith, I., (2003). "Elasto-plastic Modeling of Wood Bolted Connections," *Computers and Structures*, 81, 747-754.
- Kessel, M. H. and Augustin, R. (1995). "Load Behavior of Connections with Oak Pegs," Peavy, M.D. and Schmidt, R.J., trans. *Timber Framing, Journal of the Timber Framers Guild*. 38, December, 6-9.
- Kessel, M. H. and Augustin, R. (1996). "Load Behavior of Connections with Pegs II," Peavy, M.D. and Schmidt, R.J., trans. *Timber Framing, Journal of the Timber Framers Guild*. 39, March, 8-11.
- Patton-Mallory, M., Cramer, S.M., Smith, F.W., Pellicane, P.J., (1997). "Nonlinear Material Models for Analysis of Bolted Wood Connections." *Journal of Structural Engineering*, August, 1063-1070.
- Reid, E. H. (1997). "Behavior of Wood Pegs in Traditional Timber Frame Connections," M.S. Thesis, Michigan Technological University, Houghton, Michigan.
- Schmidt, R.J. and Daniels, C.E. (1999). "Design Considerations for Mortise and Tenon Connections," Research Report, University of Wyoming, Laramie, Wyoming.
- Schmidt, R.J. and MacKay, R.B. (1997). "Timber Frame Tension Joinery," Research Report, University of Wyoming, Laramie, Wyoming.
- Schmidt, R.J. and Scholl, G.F. (2000). "Load Duration and Seasoning Effects on Mortise and Tenon Joints," Research Report, University of Wyoming, Laramie, Wyoming.
- Sobon, J., and Schroeder, R., (1984). "Timber Frame Construction." Garden Way Publishing, Pownal, Vermont.
- Wilkinson, (1991). "Dowel Bearing Strength," FPL-RP-505, Madison, Wisconsin.
- Wood, L.W. (1951). "Relation of Strength of Wood to Duration of Load." Report 1916, Madison, Wisconsin.

9.0 Appendices

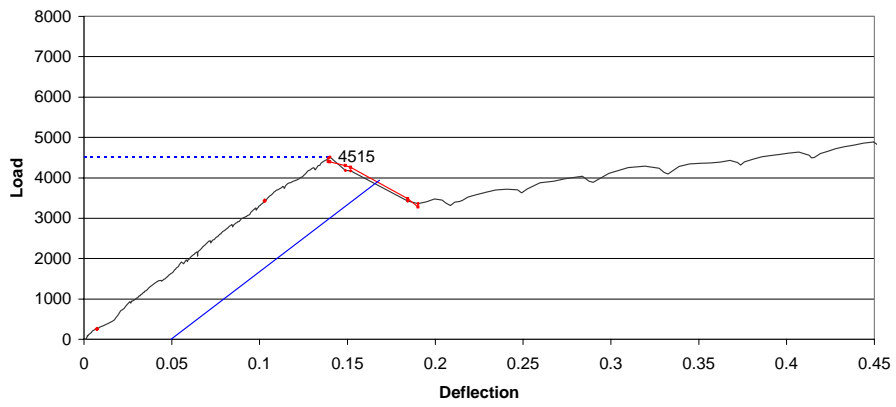
Appendix A – Tension Load-Deflection Plots



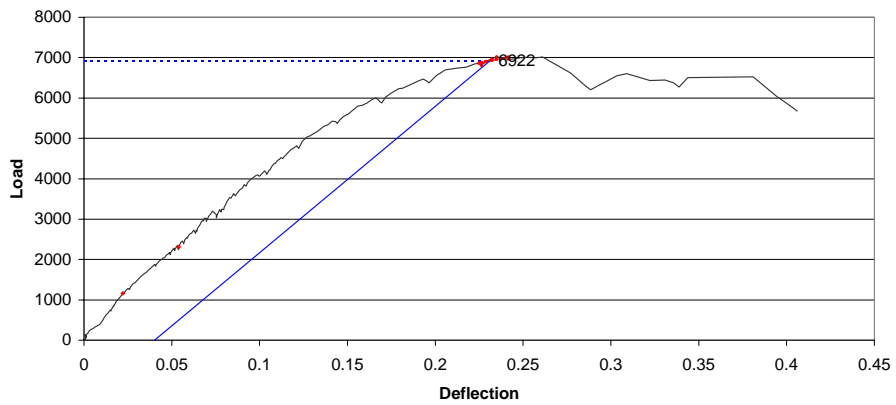
Load vs Deflection YP04



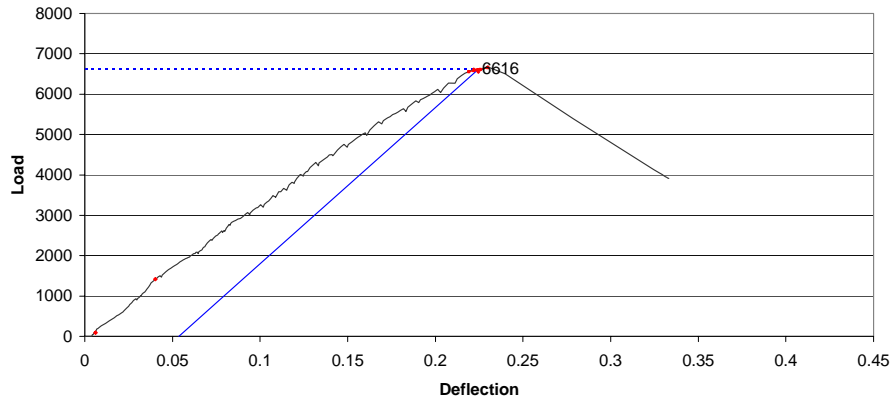
Load vs Deflection YP05



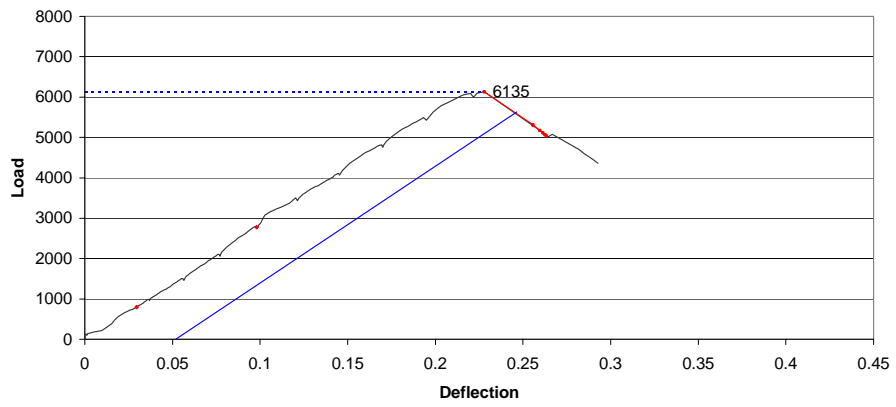
Load vs Deflection YP06



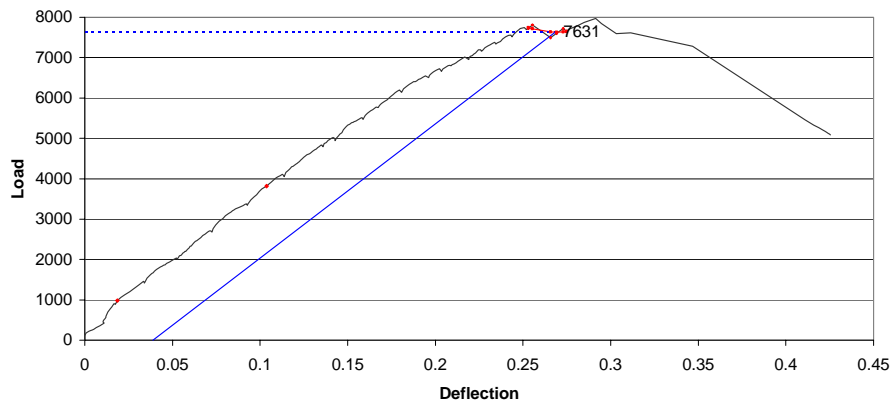
Load vs Deflection YP06B



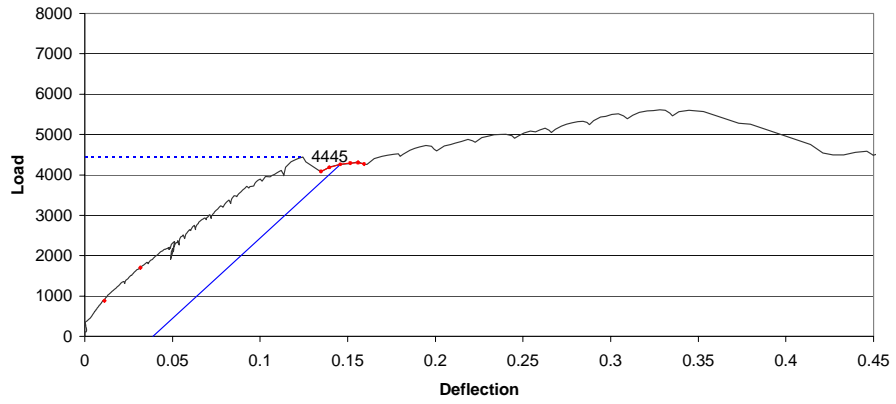
Load vs Deflection YP06C



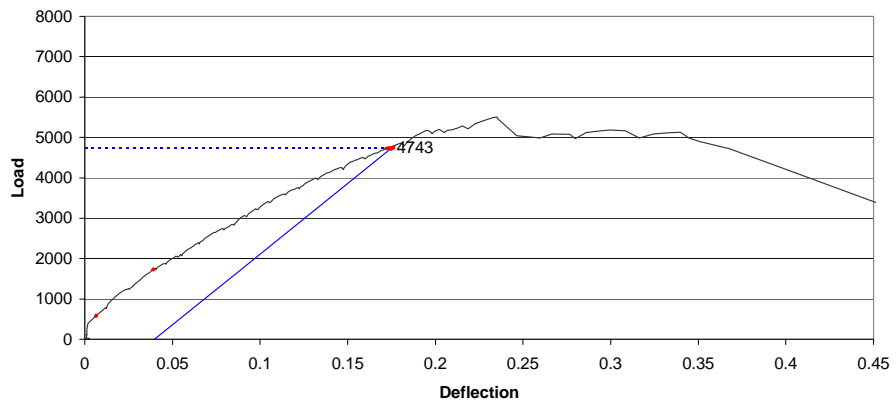
Load vs Deflection YP06D



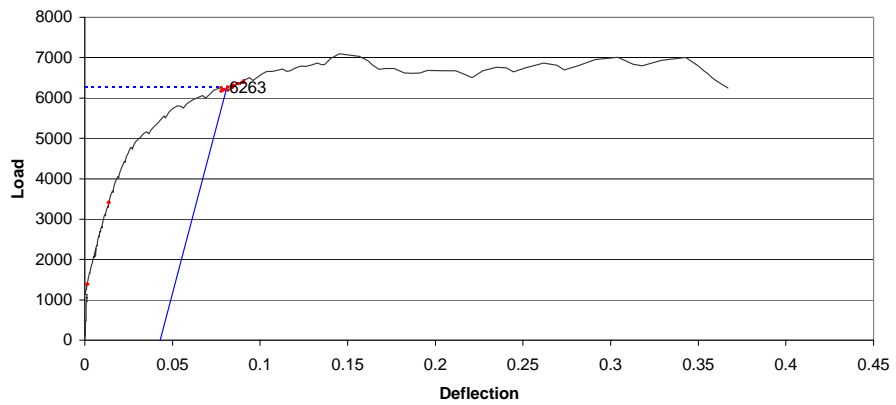
Load vs Deflection YP07



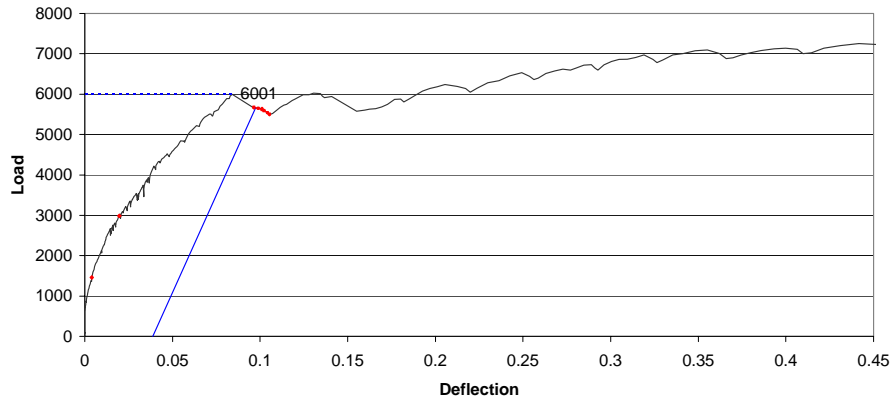
Load vs Deflection YP07B



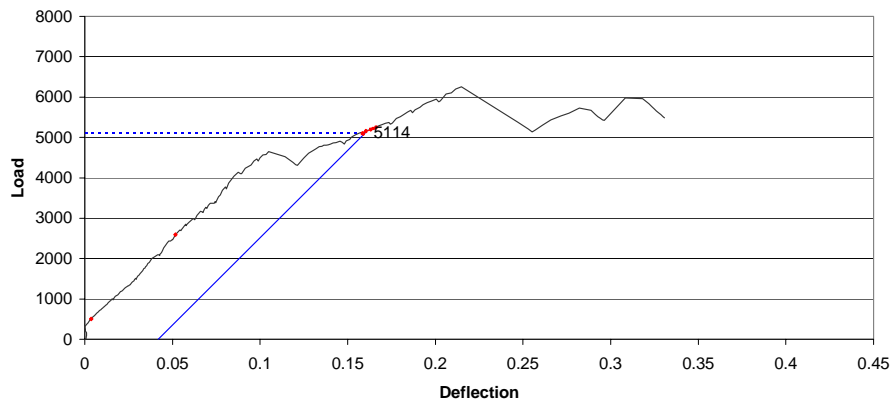
Load vs Deflection YP08



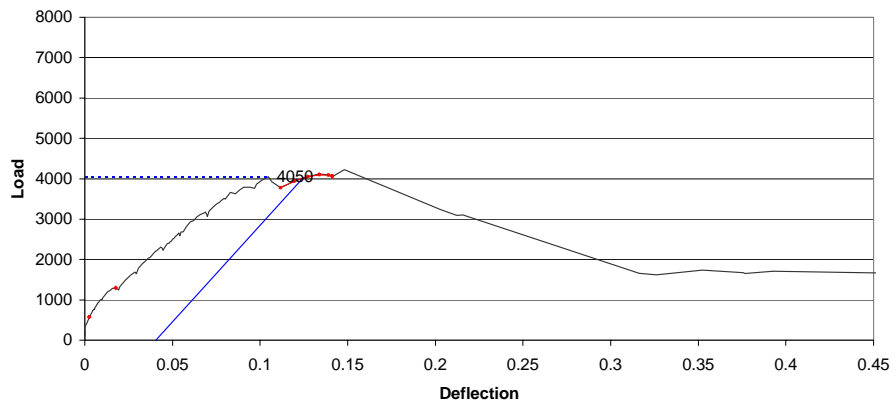
Load vs Deflection YP10



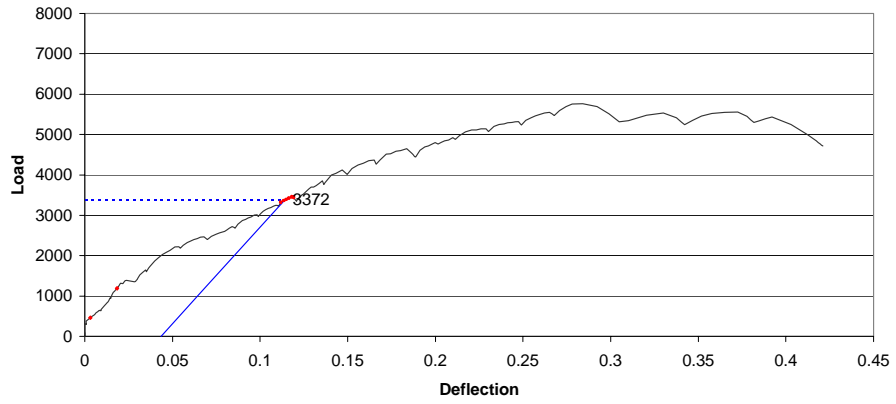
Load vs Deflection YP11



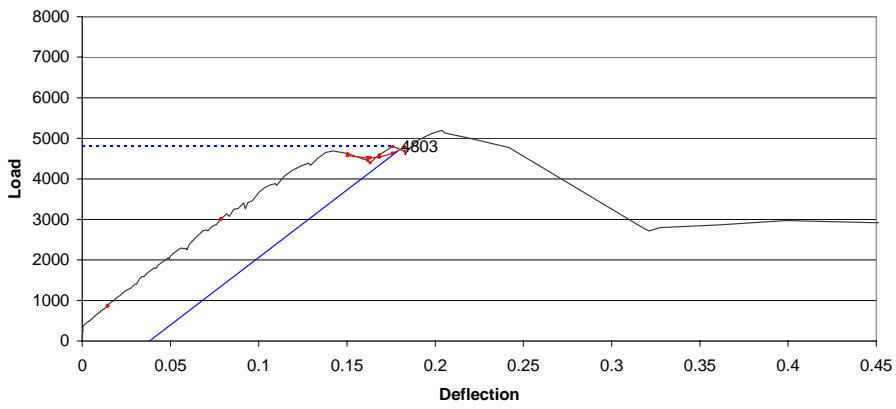
Load vs Deflection YP12



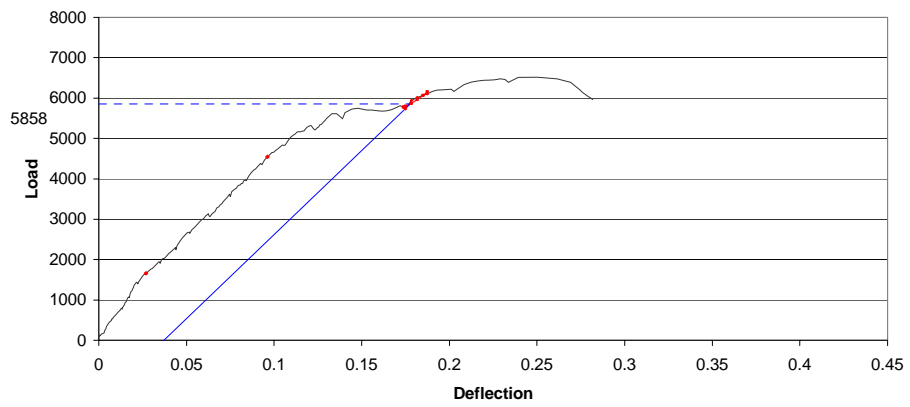
Load vs Deflection YP13



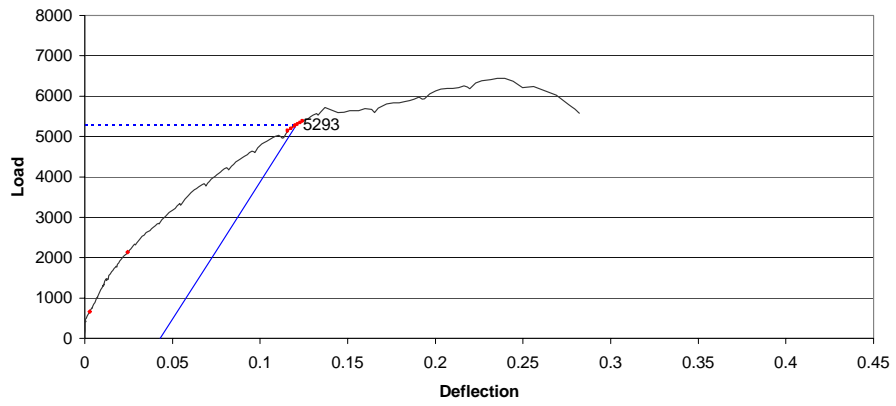
Load vs Deflection YP14



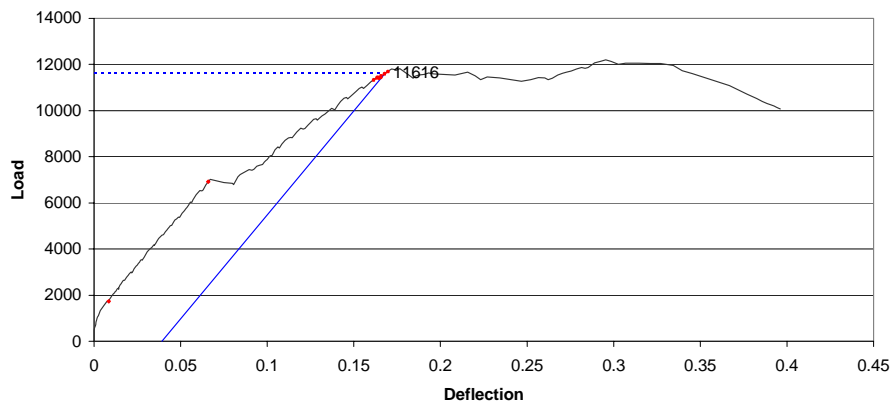
Load vs Deflection YP15



Load vs Deflection YP16

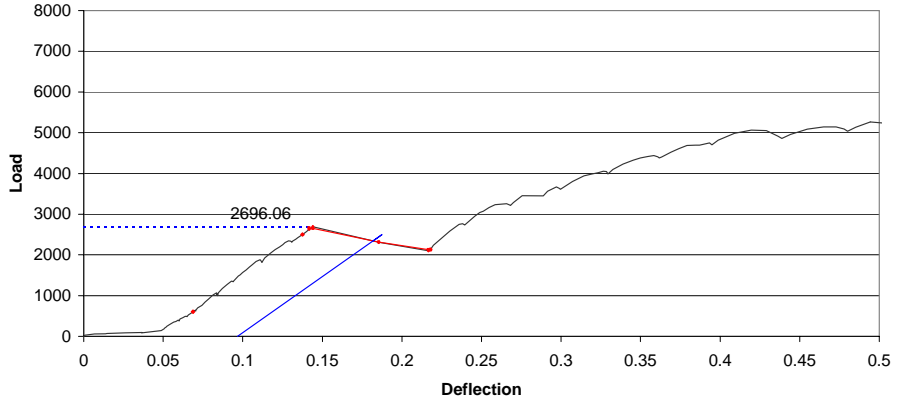


Load vs Deflection YP17

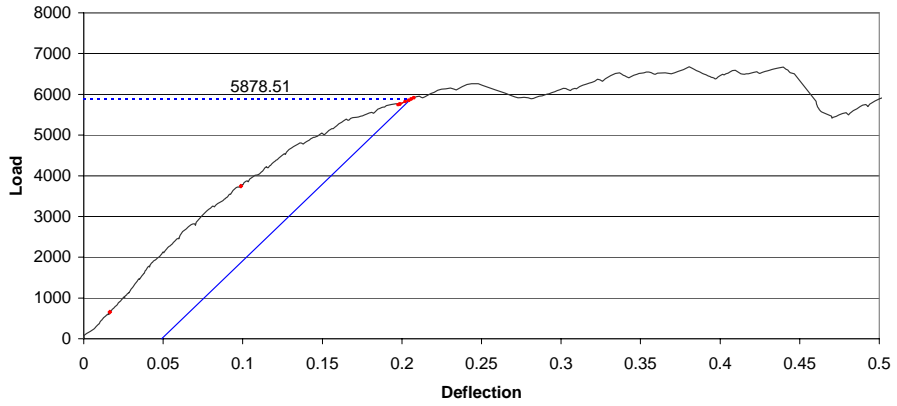


Appendix B – Shear Load Deflection Plots

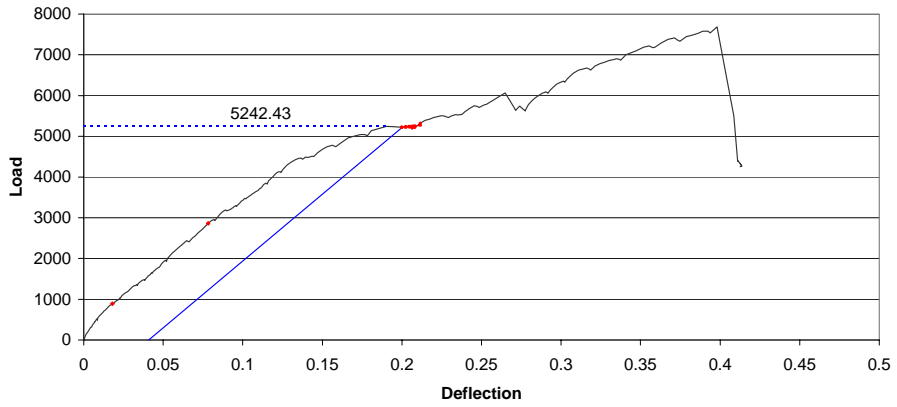
Load vs Deflection YPS01



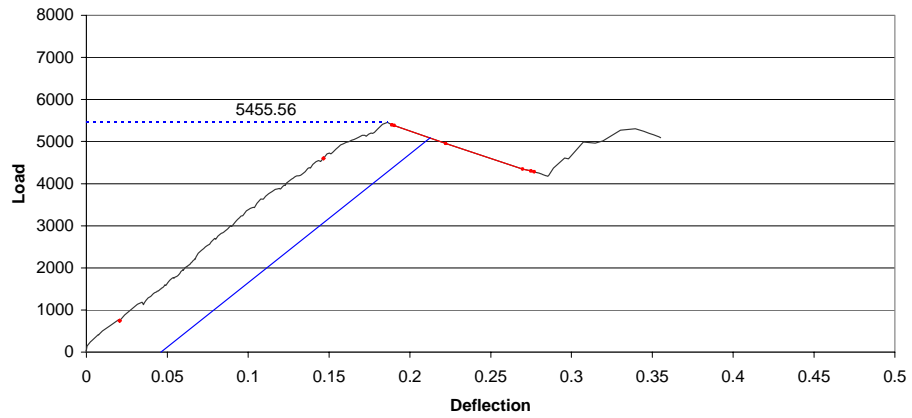
Load vs Deflection YPS02



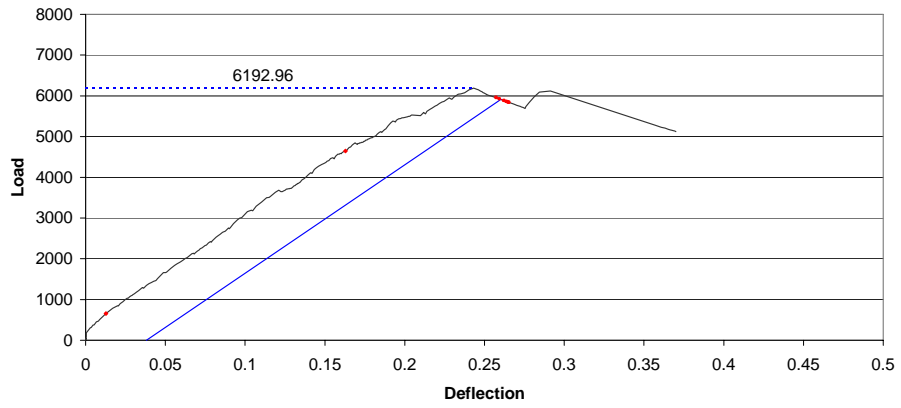
Load vs Deflection YPS03



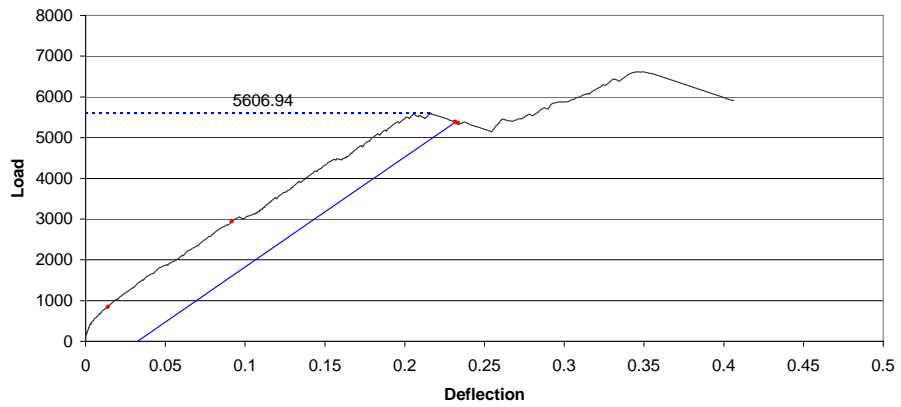
Load vs Deflection YPS04



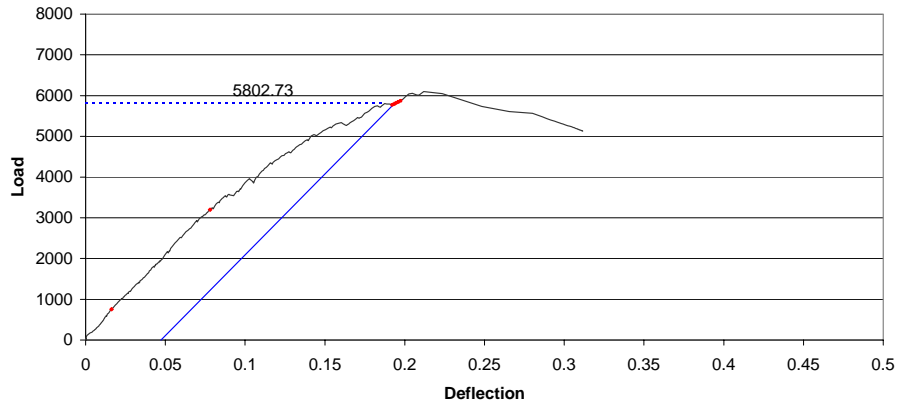
Load vs Deflection YPS04B



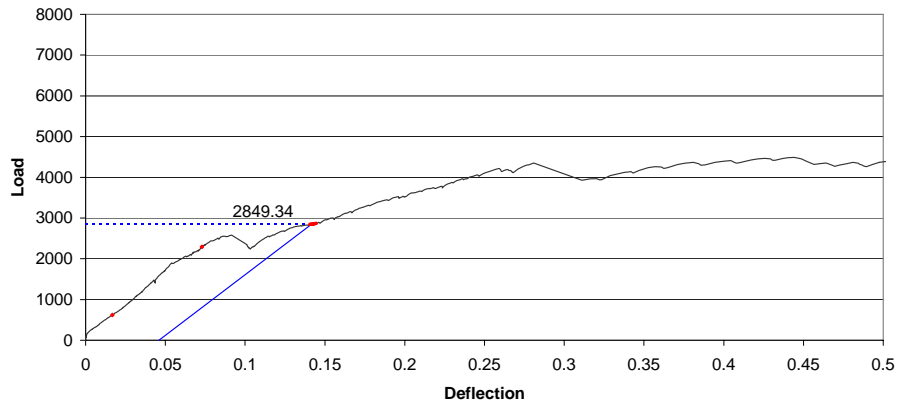
Load vs Deflection YPS04C



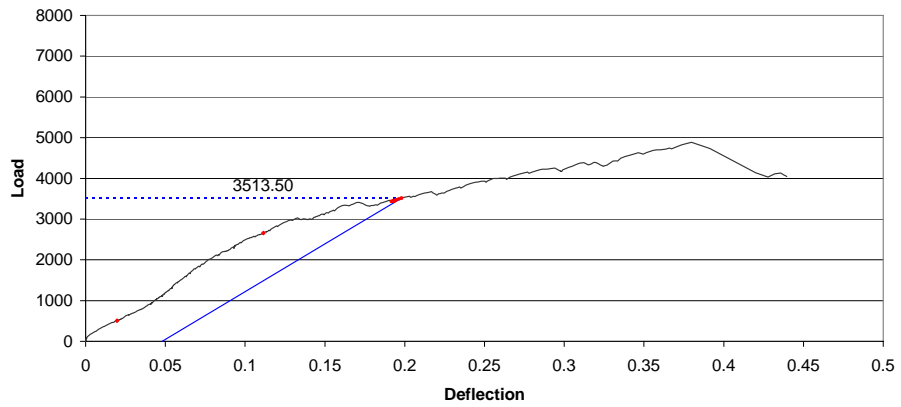
Load vs Deflection YPS05



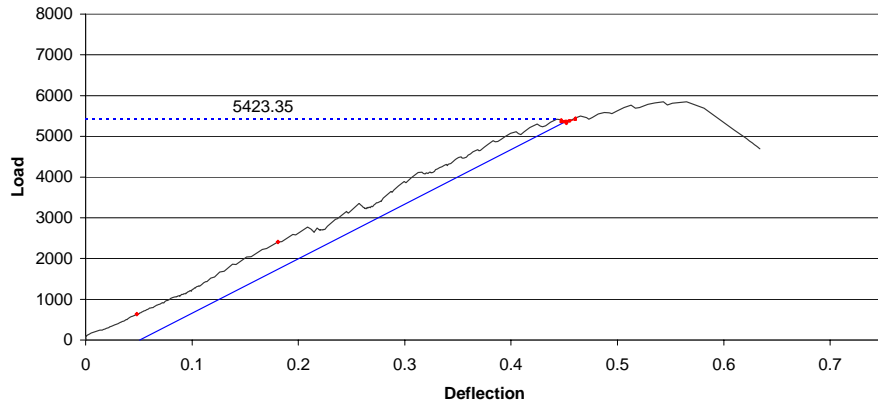
Load vs Deflection YPS06



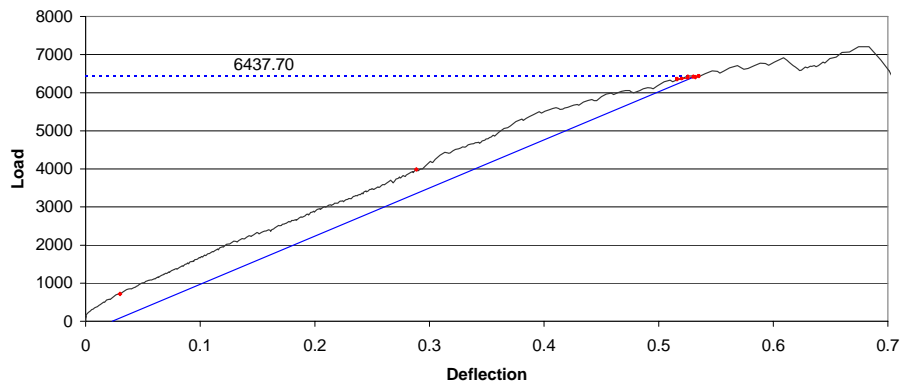
Load vs Deflection YPS07



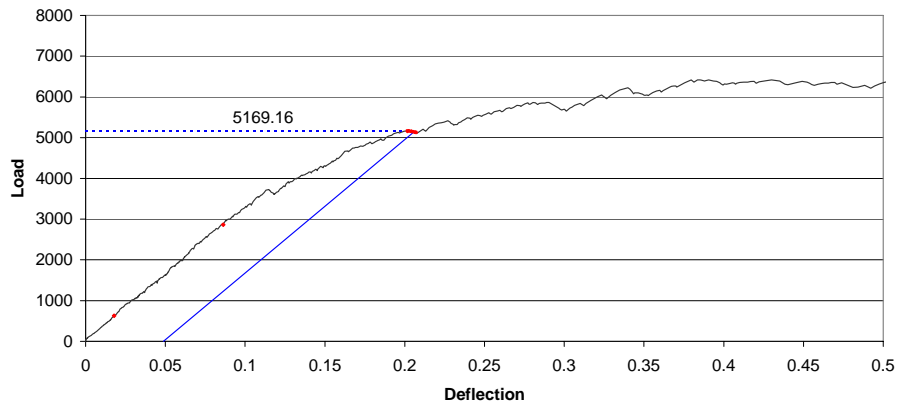
Load vs Deflection YPS07B



Load vs Deflection YPS07C

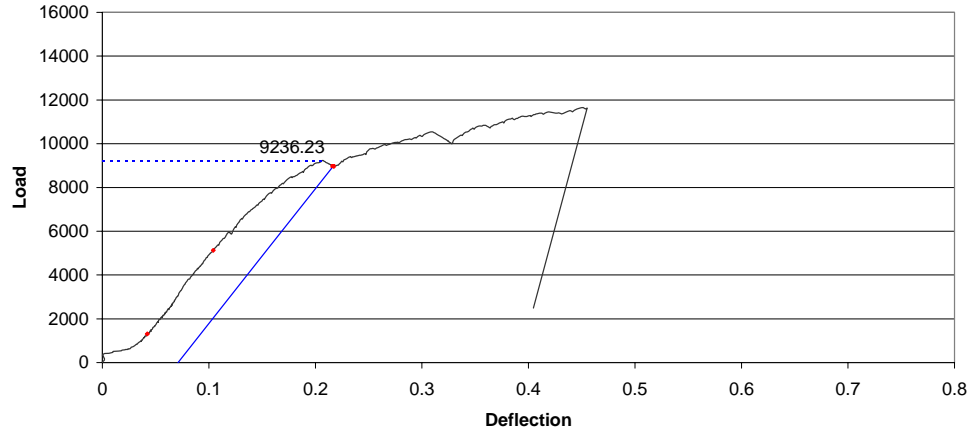


Load vs Deflection YPS08

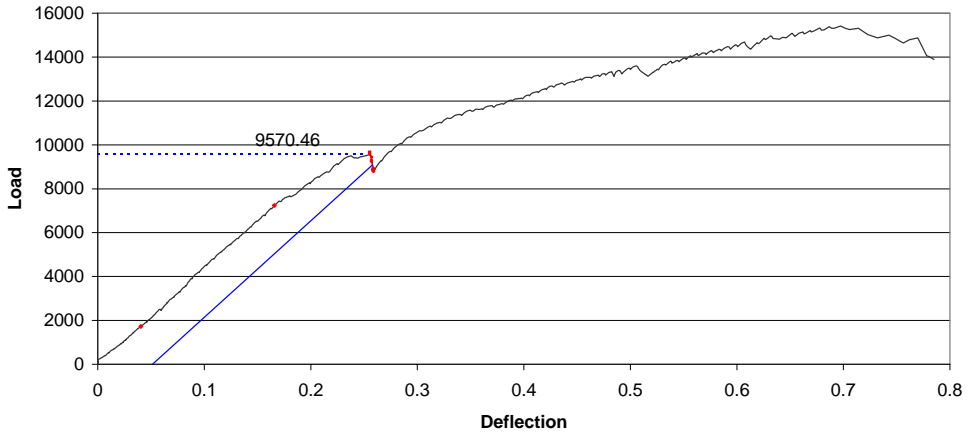


Appendix C – Direct Bearing Load-Deflection Plots

Load vs Deflection YPB01



Load vs Deflection YPB02



Appendix D – Dowel Bearing Test Data

Summary of Test Results

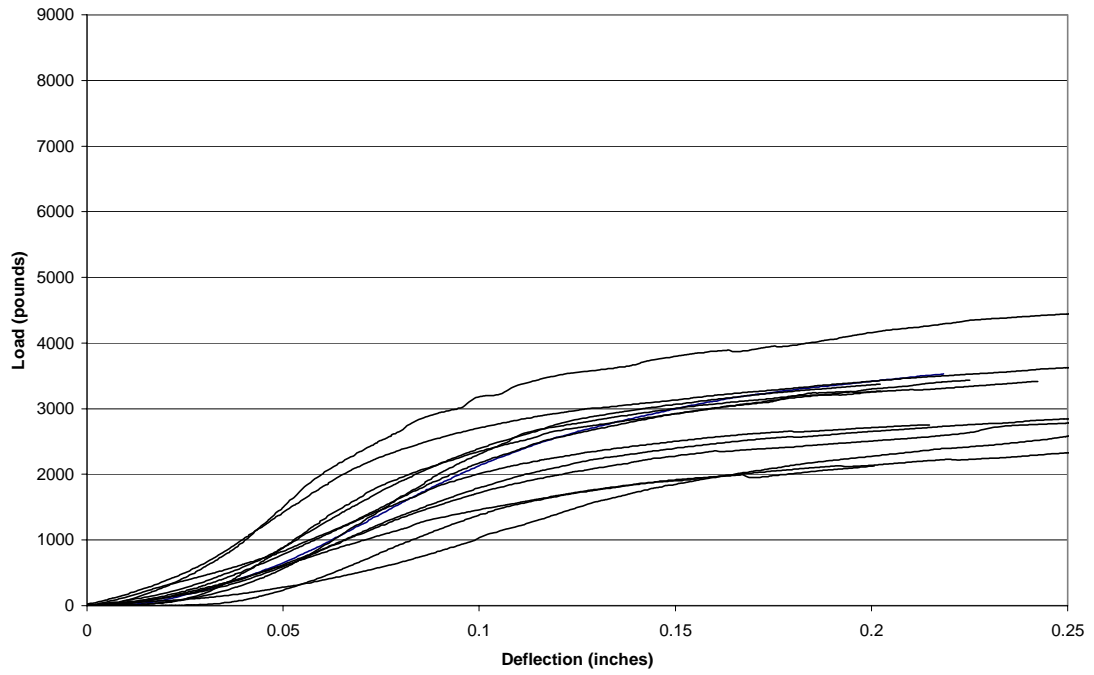
Dowel Bearing Perpendicular to the Grain in Yellow Poplar

TEST	MC	S.G.	Yield Disp. (in)	Yield Load (lb)	Stiffness (lb / in)
1	12.4%	0.471	0.190	3360	30,100
2	13.4%	0.463	0.168	3080	37,100
3	11.0%	0.441	0.143	3100	38,500
4	15.4%	0.458	0.172	3230	32,400
5	17.4%	0.403	0.179	2570	24,000
6	13.6%	0.438	0.224	2410	18,700
7	17.6%	0.435	0.145	3750	50,300
8	12.7%	0.458	0.152	2940	39,100
9	19.2%	0.398	0.179	2070	18,500
10	14.4%	0.372	0.167	1990	23,900
11	13.1%	0.401	0.175	2410	23,900
12	9.5%	0.366	0.169	2610	26,300
13	11.1%	0.430	0.181	3210	29,500
Average	0.139	0.426	0.173	2830	30,200
St. Dev	0.028	0.035	0.021	530	9200
COV	20.4%	8.1%	12.0%	18.7%	30.5%

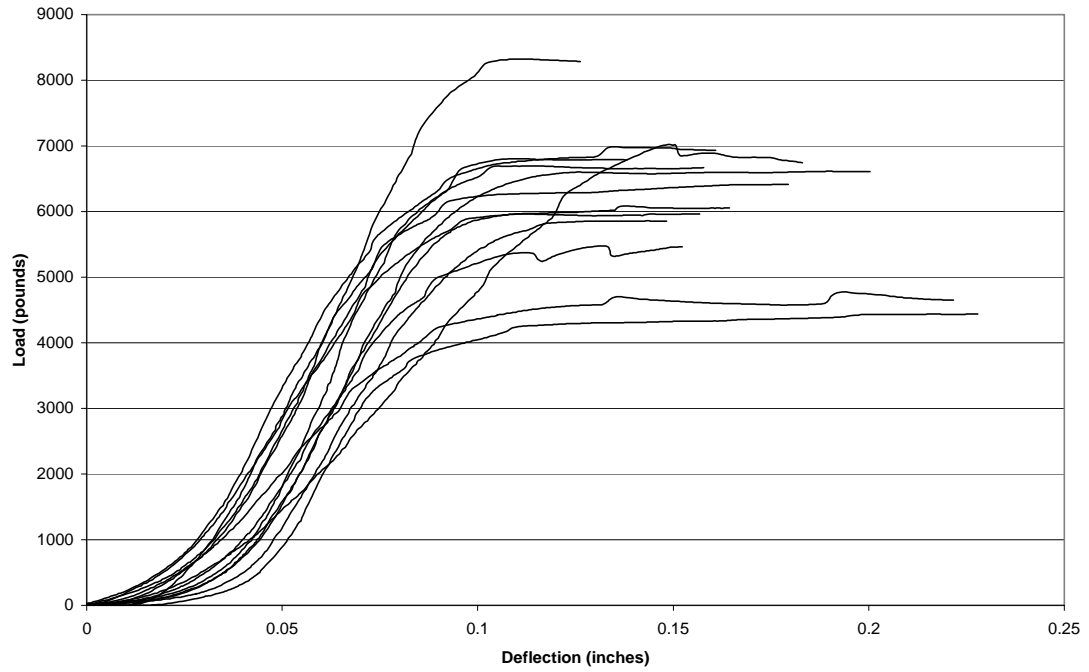
Dowel Bearing Parallel to the Grain in Yellow Poplar

TEST	MC	S.G.	Yield Disp.	Yield Load	Stiffness
1	22.1%	0.436	0.134	6040	92,100
2	12.7%	0.428	0.110	8320	135,100
3	12.9%	0.438	0.132	6920	115,200
4	15.0%	0.450	0.112	6810	111,100
5	15.0%	0.439	0.115	6700	136,500
6	12.5%	0.399	0.136	4700	70,000
7	11.5%	0.416	0.149	7020	70,000
8	19.6%	0.431	0.130	6290	113,100
9	21.3%	0.431	0.111	5960	110,700
10	11.2%	0.424	0.132	5480	92,500
11	19.5%	0.429	0.126	6600	114,400
12	19.5%	0.426	0.143	5860	102,300
13	20.8%	0.399	0.131	4300	111,200
Average	0.164	0.427	0.128	6230	105,700
St. Dev	0.041	0.015	0.012	1040	20,500
COV	24.9%	3.4%	9.8%	16.7%	19.4%

Dowel Bearing Test Perpendicular to Grain



Dowel Bearing Tests Parallel To Grain



Appendix E – Statistical Methods for Correlation

Output from MathCAD worksheet for a two-variable power fit

n := 15
i := 0..n - 1
 $\tau_i := GP_i := GB_i :=$

2288	.74	.45
1602	.64	.48
1878	.64	.48
2444	.77	.66
1610	.75	.35
1908	.66	.45
1735	.73	.43
2683	.73	.68
1416	.73	.36
2691	.73	.73
2374	.73	.51
2400	.73	.50
2480	.68	.68
1667	.68	.43
2017	.68	.51

Specific Gravity and Yield Stress Data

$\log GP_i := \log(GP_i)$

$\log \tau_i := \log(\tau_i)$

$\log GB_i := \log(GB_i)$

$\tau\text{bar} := \sum_i \log \tau_i$

$GP\text{sbar} := \sum_i (\log GP_i)^2$

$GP\text{bar} := \sum_i \log GP_i$

$GB\text{sbar} := \sum_i (\log GB_i)^2$

$GB\text{bar} := \sum_i \log GB_i$

$GPGB\text{bar} := \sum_i \log GP_i \cdot \log GB_i$

$GP\tau\text{bar} := \sum_i \log GP_i \cdot \log \tau_i$

Converting to a Linear Function

Creating Normal Terms

$$GB\bar{\tau} := \sum_i \log GB_i \cdot \log \tau_i$$

$$A := \begin{pmatrix} n & GP\bar{b} & GB\bar{b} & \bar{\tau} \\ GP\bar{b} & GP\bar{s} & GPGB\bar{b} & GP\bar{\tau} \\ GB\bar{b} & GPGB\bar{b} & GB\bar{s} & GB\bar{\tau} \end{pmatrix}$$

$$SOL := rref(A)$$

$$a1 := SOL_{1,3}$$

$$a0 := SOL_{0,3}$$

$$a2 := SOL_{2,3}$$

$$a0 := 10^{a0}$$

$$fn(GP, GB) := a0 \cdot GP^{a1} \cdot GB^{a2}$$

$$a0 = 4.809 \times 10^3$$

$$a1 = 0.926$$

$$a2 = 0.778$$

$$St := \sum_i (\tau_i)^2 - \frac{\left(\sum_i \tau_i\right)^2}{n}$$

$$St = 2.516 \times 10^6$$

$$Sr := \sum_i \left[\tau_i - a0 \cdot (GP_i)^{a1} \cdot (GB_i)^{a2} \right]^2$$

$$St = 2.516 \times 10^6$$

$$r := \sqrt{\frac{St - Sr}{St}}$$

$$r^2 = 0.80295244$$

$$S := \text{CreateMesh}(fn, .6, .8, .3, .8, 10)$$

Solving Normal Matrix

Converting back to Power Function

Least Squares Regression

